Stratigraphic record of Pleistocene faulting and basin evolution in the Borrego Badlands, San Jacinto fault zone, Southern California

Andrew T. Lutz
Rebecca J. Dorsey†
Department of Geological Sciences, 1272 University of Oregon, Eugene, Oregon 97403-1272, USA

Bernard A. Housen
Department of Geology, Western Washington University, Bellingham, Washington 98225-9080, USA

Susanne U. Janecke
Department of Geology, Utah State University, Logan, Utah 84322-4505, USA

ABSTRACT

Sedimentary rocks in the Borrego Badlands, Southern California, contain a record of Pleistocene crustal deformation during initiation and evolution of the San Jacinto fault zone. We used detailed geologic, stratigraphic, and paleomagnetic analysis to determine the age and geometry of the deposits and reconstruct the history of fault-controlled sedimentation in this area. The base of the ~300 to 500 m thick Ocotillo Formation is a paraconformity to abrupt conformable contact that records a brief hiatus followed by rapid progradation of coarse alluvial sediment over lacustrine facies of the Borrego Formation at 1.05 ± 0.03 Ma. This coincides with regional-scale progradation of Ocotillo Formation sand and gravel, and appears to record initiation of strike-slip faults in the southwestern Salton Trough at ca. 1.1 Ma. Thickness trends, clast compositions, paleocurrents, and distribution of paleosols provide evidence for initiation of the East Coyote Mountain fault at ca. 1.05 Ma, followed by onset of NNE-ward basin tilting obliquely toward the Santa Rosa segment of the Clark fault at ca. 1.0 Ma. Stratigraphic omission of the Ocotillo Formation and progressively older units southwest of the Coyote Creek fault beneath the Fonts Point Sandstone provides evidence that tilting to the north-northeast was related in part to growth of the San Felipe anticline during deposition of the Ocotillo Formation. Map and stratigraphic data suggest that the Coyote Creek fault in the western Borrego Badlands postdates Ocotillo deposition, and thus appears to have propagated southeast into the study area at ca. 0.6 Ma.

The Fonts Point Sandstone is a thin, sheet-like alluvial deposit that records the end of deposition and onset of transpressive deformation in the Borrego Badlands. The base of the Fonts Point Sandstone changes from a conformable contact in a narrow belt southeast of the Inspiration Point fault, where it is dated at 0.6 ± 0.02 Ma, to an angular unconformity on the folded Ocotillo Formation northwest of the fault. The pattern of stratal truncation records initiation of the Inspiration Point fault at ca. 0.6 Ma. This coincides with a major structural reorganization in the San Jacinto fault zone that initiated the modern phase of north-south shortening and erosion in the southwestern Salton Trough.

Keywords: stratigraphy, San Jacinto fault, Pleistocene, California, basin analysis.

INTRODUCTION

The San Andreas fault system in Southern California is a complicated zone of active strike-slip faults and related crustal deformation that accommodates ~50 mm/yr of relative motion between the Pacific and North American plates (Fig. 1) (DeMets et al., 1990; Bennett et al., 1996; DeMets and Dixon, 1999; McCaffrey, 2005; Meade and Hager, 2005). While the location and seismic expression of faults in this zone are relatively well known, the partitioning of strain in space and time, and the long-term evolution of faults at geologic time scales (10^6 yr), remain poorly understood. Stratigraphy provides a useful tool for documenting changes in the position and behavior of basin-bounding faults through time, because it records dynamic interactions between subsidence and sediment input that are commonly controlled by faulting in tectonically active regions (e.g., Paola et al., 1992; Gawthorpe et al., 1994, 1997; Paola, 2000). Thus we can use our knowledge of tectonic controls on stratigraphic evolution to better understand the late Cenozoic evolution of the San Andreas fault system in the western Salton Trough.

The western Salton Trough contains over 6 km of upper Miocene to Pleistocene sedimentary rocks that record crustal deformation and basin subsidence during evolution of the San Andreas plate-boundary system in Southern California (Dibblee, 1954, 1984, 1996; Woodard, 1963, 1974; Kerr, 1982; Winker, 1987; Kerr and Kidwell, 1991; Winker and Kidwell, 1996). Recent studies have shown that, from late Miocene to early Pleistocene time, formation of this basin was controlled by combined slip on the San Andreas fault in the northeast and the West Salton detachment fault in the west (Axen and Fletcher, 1998; Dorsey, 2006; Steely, 2006; Kirby et al., in press). The change from regional transtension and detachment faulting to strike-slip faulting and transpression resulted from a major tectonic reorganization in late Pliocene or early Pleistocene time, but the timing and style of this transition are poorly understood. As a result, our understanding of Pliocene-Pleistocene regional kinematics and plate-boundary deformation in Southern California is limited.

This paper documents the stratigraphy and architecture of the Pleistocene Ocotillo Formation and Fonts Point Sandstone in the Borrego Badlands, near the western margin of the Salton Trough (Fig. 1). A thick sequence of alluvial,

†Corresponding author e-mail: rdorsey@uoregon.edu.

GSA Bulletin; November/December 2006; v. 118; no. 11/12; p. 1377–1397; doi: 10.1130/B25946.1; 15 figures; 1 table, Data Repository item 2006217.

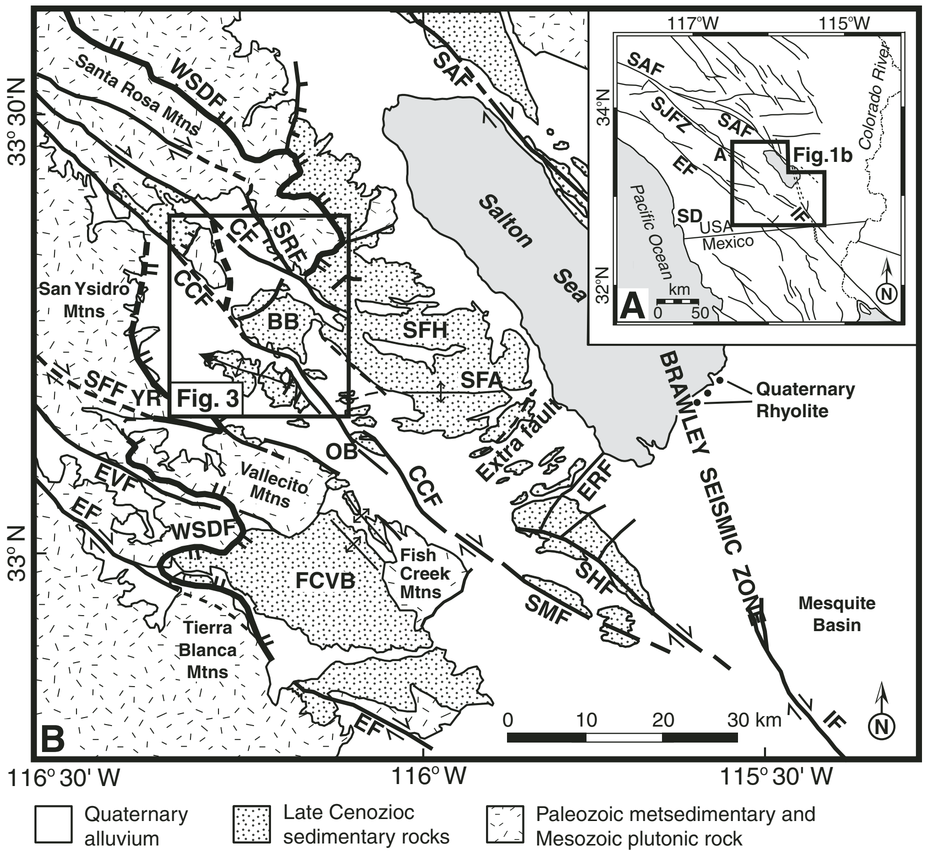

Figure 1. (A) Fault map of Southern California, modified from Sharp (1967). (B) Generalized geologic map of the western Salton Trough. A—Anza; BB—Borrego Badlands; CCF—Coyote Creek fault; CF—Clark fault; EF—Elsinore fault; ERF—Elmore Ranch fault; EVH—Earthquake Valley fault; FCVB—Fish Creek–Vallecito basin; IF—Imperial fault; OB—Ocotillo Badlands; SAF—San Andreas fault; SD—San Diego; SFA—San Felipe anticline; SFF—San Felipe fault; SFH—San Felipe Hills; SHF—Superstition Hills fault; SJFZ—San Jacinto fault zone; SMF—Superstition Mountain fault; SRF—Santa Rosa fault; WSDF—West Salton detachment fault; YR—Yaqui Ridge. Adapted from a map originally compiled by L. Seeber, modified after Axen and Fletcher (1998), Steely (2006), Kirby et al. (in press), Kirby (2005).

fluvial, and lacustrine sediments in this area records crustal tilting and sedimentation that took place between the modern traces of the Clark and Coyote Creek faults. Detailed study of these deposits provides new information about the timing and style of faulting that controlled Pleistocene sedimentation in the Borrego Badlands. Comparison with companion studies in the San Felipe Hills (Kirby, 2005; Kirby et al., in press) and northern Vallecito Mountains (Steely et al., 2005; Steely, 2006) suggests that widespread progradation of the Ocotillo Formation at ca. 1.1 Ma records initiation of several dextral strike-slip faults in the western Salton Trough. Stratigraphic and structural data from the Borrego Badlands (this study) are useful for testing and refining the age of this young fault zone, and provide evidence for early slip on the San Jacinto fault zone in the Salton Trough.

GEOLOGIC BACKGROUND

Regional Stratigraphy

The western Salton Trough is a structurally complex region of fault-bounded basement uplifts and flanking sedimentary basins (Fig. 1) that formed in response to late Cenozoic rifting and transtensional strain adjacent to the San Andreas fault (e.g., Dibblee, 1954; Woodard, 1963; Winker, 1987; Winker and Kidwell, 1996). Pliocene-Pleistocene sedimentary basins in this region can be divided into two subbasins: the Fish Creek–Vallecito basin in the south, and the San Felipe–Borrego basin (San Felipe Hills and Borrego Badlands) in the north (Fig. 1) (Dorsey et al., 2005). During most or all of Pliocene time, the two subbasins were part of a single large supradetachment basin that formed in the hanging wall of the West Salton detachment fault system (e.g., Axen and Fletcher, 1998; Dorsey, 2006). This large basin was segmented into two separate subbasins by initiation of the intervening dextral-normal San Felipe fault zone, perhaps as recently as ca. 1.1 Ma (Kirby, 2005; Kirby et al., in press; Steely et al., 2005; Steely, 2006).

Upper Miocene to Pleistocene sedimentary rocks in the western Salton Trough record initiation, evolution, and deactivation of the West Salton detachment fault system (Fig. 2). Older deposits overlie crystalline basement that includes Cretaceous tonalite and granodiorite, pre-Cretaceous metasedimentary rocks, and Late Cretaceous mylonite formed by regional top-to-the-west thrusting (Sharp, 1967; Dibblee, 1954; Jahns, 1954; Gastil, 1975; Engel and Schultejann, 1984; Calzia et al., 1988; Simpson, 1984). Upper Miocene, rift-related nonmarine deposits of the Split Mountain Group are locally preserved and are overlain by widespread marine strata of the lower Pliocene Imperial Formation (Woodard, 1963; Dibblee, 1954; Kerr, 1982; Winker, 1987; Kerr and Kidwell, 1991; Winker and Kidwell, 1996; Dorsey et al., in press).

The Pliocene Palm Spring Formation was originally described by Woodard (1963) and was later redefined as a group that includes the Diablo and Olla Formations, Canebrake Conglomerate, and Borrego Formation (Winker and Kidwell, 1996). The Diablo Formation is 1–2 km thick and contains Colorado River–derived fluvial-deltaic sandstone and mudstone that pass laterally into coarse basin-margin facies of the Olla Formation and Canebrake Conglomerate (Dibblee, 1954; Morley, 1963; Hoover, 1965; Reitz, 1977; Winker, 1987; Winker and Kidwell, 1996). Sandstone units represent deposits of a meandering channel system, and siltstone and claystone are interpreted as overbank facies, similar to deposits of the modern Colorado River delta system in the Salton Trough (Dibblee, 1954; Winker, 1987).

The Borrego Formation is a thick, regionally extensive unit of lacustrine claystone, mudstone, and marlstone with minor sandstone and siltstone that overlies and is in part laterally equivalent to the Diablo Formation (Fig. 2) (Tarbet and Holman, 1944; Dibblee, 1954, 1984; Morley, 1963; Bartholomew, 1968; Dronyk, 1977; Reitz, 1977; Wagoner, 1977; Ferragen, 1986; Winker, 1987; Wells, 1987; Dorsey et al., 2005; Kirby, 2005; Kirby et al., in press). The age of the basal contact of the Borrego Formation in the San Felipe–Borrego basin is probably time-transgressive and is generally considered to be middle or late Pliocene (Woodard, 1963). Ostracodes (*Chara*, *Rotalia beccarii*, *Elphidium*), gastropods, fish bone fragments,

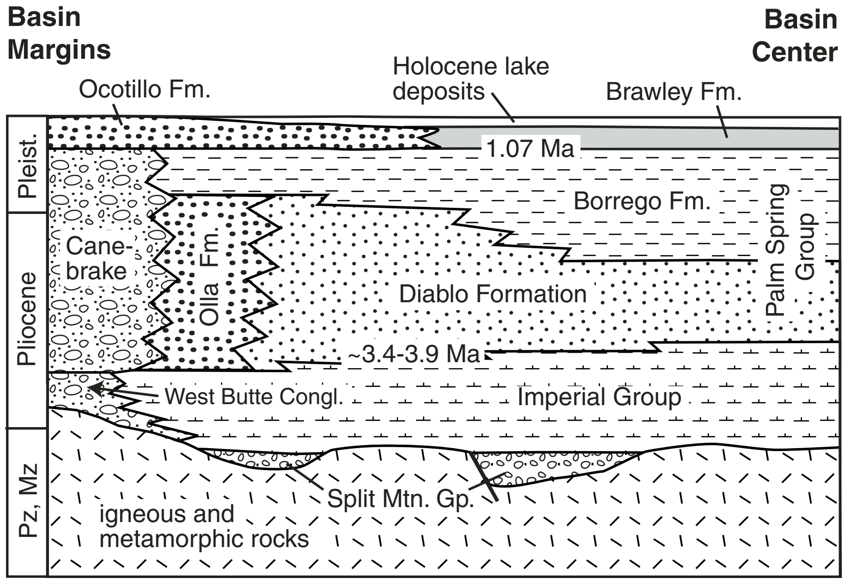

Figure 2. Stratigraphy of the San Felipe–Borrego basin in the western Salton Trough, modified from Dibblee (1954), Reitz (1977), and Steely (2006). Age of the Palm Spring Group is based on micropaleontologic study of Quinn and Cronin (1984). Age of the base of the Ocotillo Formation is based on paleomagnetic studies discussed in text, including this study.

calcareous algae, forams, micromollusks, and charophytes in the Borrego Formation indicate deposition in a large perennial lake (Tarbet and Holman, 1944; Dibblee, 1954; Dronyk, 1977; Wagoner, 1977; Kirby et al., in press). Sandstone composition records input from both local and Colorado River sources (Guthrie, 1990). The Borrego Lake basin was filled with water during most of Borrego time, and only rarely experienced lake-level lowstands as recorded in erosion-based channel-fill conglomerate and sandstone (Kirby, 2005; Kirby et al., in press; R. Dorsey, unpub. data).

The Ocotillo Formation is a regionally extensive unit of alluvial sedimentary rocks that overlie the Borrego Formation along a contact that varies laterally in the San Felipe–Borrego basin from conformable and interbedded to a disconformity and angular unconformity (Dibblee, 1954, 1984, Bartholomew, 1968, 1970; Brown et al., 1991; Kirby, 2005; Kirby et al., in press; this study). The age of the Ocotillo Formation is known to range from ca. 1.1 Ma at the base to ca. 0.5 Ma at the top, based on paleomagnetic studies in the Ocotillo Badlands (Brown et al., 1991), southeastern San Felipe Hills (Kirby, 2005; Kirby et al., in press), and the Borrego Badlands (Remeika and Beske-Diehl, 1996; this study). Its age is further constrained in the Borrego Badlands by the presence of the 0.76 Ma Bishop ash, 0.74 Ma Thermal Canyon ash, and abundant Irvingtonian vertebrate fossils (Remeika and Jefferson, 1993; Jefferson and Remeika, 1994; Remeika and Beske-Diehl, 1996; Bell et al., 2004; Remeika, 2006).

The Brawley Formation is the fine-grained distal equivalent of the Ocotillo Formation in the western Salton Trough (Fig. 2) (Dibblee, 1954; Kirby, 2005; Kirby et al., in press). Previous workers concluded that the Brawley Formation is indistinguishable from the lacustrine Borrego Formation, but Kirby (2005) showed that the Brawley Formation in the San Felipe Hills contains abundant fluvial and eolian sandstone interbedded with lake-margin mudstone, making it coarser and lithologically distinct from the underlying Borrego Formation. Detailed sedimentologic study of these units shows that an abrupt change occurred at ca. 1.07 Ma, from perennial lacustrine conditions of the Borrego Formation to fluvial-deltaic and lacustrine sedimentation with frequent desiccation episodes (Brawley Formation) (Kirby, 2005; Kirby et al., in press).

San Felipe Anticline

The San Felipe anticline is a large, EW-trending fold in the southern San Felipe Hills (Fig. 1B) that was first mapped and interpreted by Dibblee (1954, 1984). Geologic mapping and gravity analysis show that a significant E-trending gravity high coincides closely with the surface trace of the anticline, indicating that crystalline basement rock occupies the core of the fold at depth (Kirby, 2005; Kirby et al., in press). Systematic truncation of older units below an angular unconformity at the base of the Ocotillo Formation, combined with lack of growth relationships in the upper Borrego Formation, provides evidence that fold growth initiated at ca. 1.1 Ma immediately prior to widespread progradation of the Ocotillo and Brawley Formations across the southwestern Salton Trough (Kirby, 2005; Kirby et al., in press). The San Felipe anticline is truncated and offset by the right-lateral Coyote Creek fault (Fig. 1B), and southwest of the fault the fold trend is less certain because the Pleistocene fold is developed in the same areas as an older Pliocene NW-trending anticline (Fig. 3) (Steely, 2006). Stratigraphic and map relationships summarized below indicate that the area from Borrego Mountain to the northern Borrego Badlands experienced broad north-northeast tilting on the north limb of the San Felipe anticline during deposition of the Ocotillo Formation (Kirby, 2005; Kirby et al., in press; this study).

San Jacinto Fault Zone

The San Jacinto fault zone is a young strand of the southern San Andreas fault system in Southern California (Figs. 1 and 3). It is a group of seismically active, complexly linked strike-slip fault segments that merge with the San Andreas fault in the northwest and the Imperial fault in the southeast (Sharp, 1967; Sanders, 1989; Morton and Matti, 1993; Sanders and Magistrale, 1997; Dorsey, 2002; Ryter, 2002; Janecke et al., 2005; Dorsey and Roering, 2006) (Fig. 1A). Estimates of the age of the fault zone vary from ca. 1.0 to 2.4 Ma, based on evidence from stratigraphic and structural studies in the San Bernardino area (Matti and Morton, 1993; Morton and Matti, 1993; Kendrick et al., 2002) and as inferred from extrapolation of late Quaternary slip rates near Anza (Sharp, 1981; Merifield et al., 1989; Rockwell et al., 1990).

Sharp (1967) measured ~22–24 km of total dextral offset on the San Jacinto fault zone based on correlation of Cretaceous pluton margins and Late Cretaceous mylonite. In and near the study area, the San Jacinto fault zone contains two through-going active faults, the Clark and Coyote Creek faults, which cut Pleistocene sedimentary rocks in the Borrego Badlands (Fig. 3). The Clark fault is commonly inferred to terminate into a diffuse array of discontinuous small strands east of the Borrego Badlands, converting ~15 km of lateral displacement into a zone of intensely folded sedimentary rocks (Dibblee, 1954; Sharp, 1967; Sanders, 1989). However, Kirby (2005) and Kirby et al. (in press) demonstrated with geologic mapping, structural analysis, and geophysical data sets that strong transpressional deformation and dextral fault-

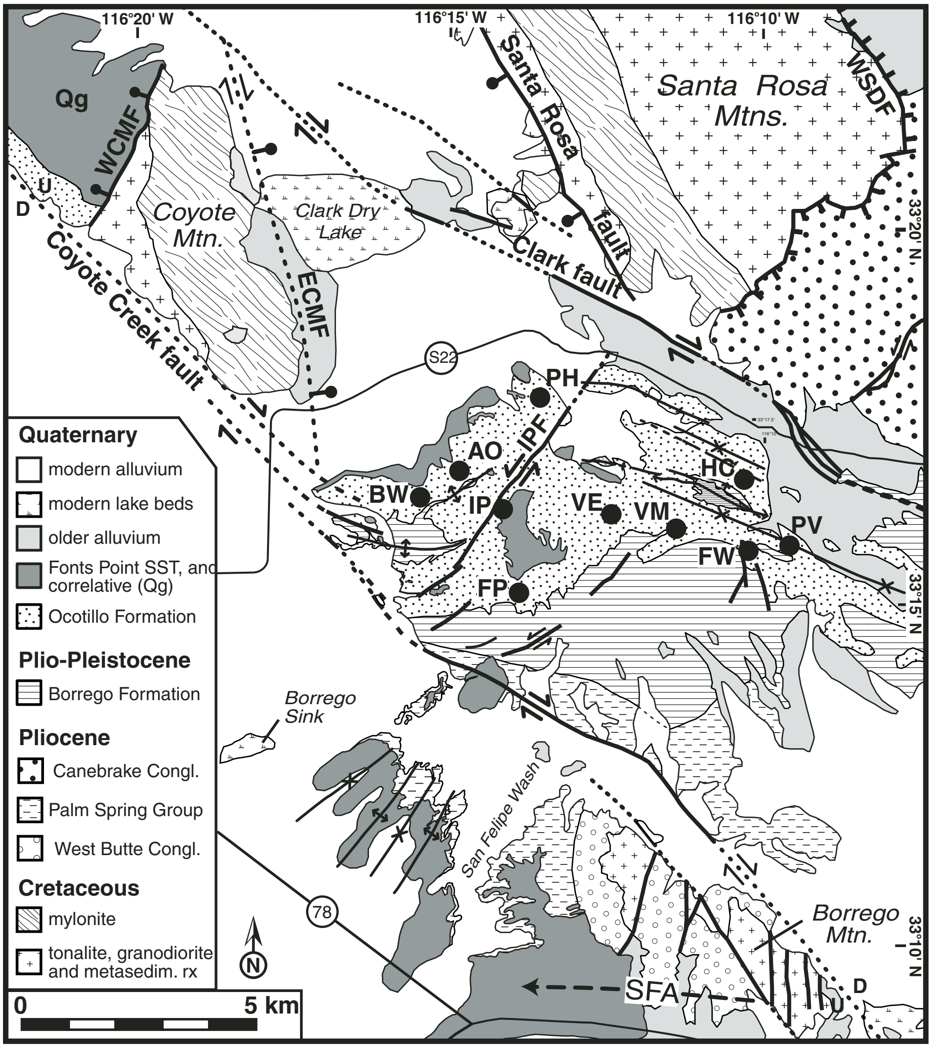

Figure 3. Generalized geologic map of the Borrego Badlands and surrounding areas. ECMF—East Coyote Mountain fault; IPF—Inspiration Point fault; SFA—San Felipe anticline; WCMF—West Coyote Mountain fault; WSDF—West Salton detachment fault (after Axen and Fletcher, 1998). Labeled dots show location of measured sections (see Figs. 4 and 7). Adapted from Rogers (1965), Dorsey (2002), Ryter (2002), Lutz (2005), Steely (2006). AO—Arroyo Otro; BW—Beckman Wash; FP—Fonts Point; FW—Fault Wash; HC—Hidden Canyon; IP—Inspiration Point; PH—Painted Hill; PV—Palo Verde Wash; VE—Valle Escondido; VM—Vista del Malpais; SST—sandstone; metasedim. rx—metasedimentary rocks.

ing extends southeast beyond the previously recognized surface tip of the Clark fault into the southeastern San Felipe Hills (Fig. 1B) (Dibblee, 1954, 1984; Sanders, 1989; Sanders and Magistrale, 1997). Bartholomew (1968, 1970) suggested that a fault segment west of the Borrego Badlands may have acted as a hard link between the Clark and Coyote Creek faults during Pleistocene time. This segment was mapped and named the Coyote Mountain fault by Theodore and Sharp (1975) on the east flank of Coyote Mountain, northwest of the study area (Fig. 3). We rename it the East Coyote Mountain fault to distinguish it from another fault west of Coyote Mountain. Evidence for the East Coyote Mountain fault includes the linear range front, a degraded inactive fault scarp (Ryter, 2002), a gravity low east of its trace (Bartholomew, 1970; Langenheim and Jachens, 1993; Martin, 1999), and the location of the internally drained Clark Dry Lake immediately adjacent to the fault.

Borrego Badlands

The Borrego Badlands occupy an area of present-day broad uplift within the modern San Jacinto fault zone that is characterized by rapidly eroding gullies and abundant exposures of Pleistocene sedimentary rocks (Figs. 3, 4, and 5). In the northern Borrego Badlands, diverse lithofacies of the Ocotillo Formation are widely exposed and deformed by active strike-slip faults and related folds (Lutz, 2005). The NE-striking left-lateral Inspiration Point fault cuts all units older than recent alluvium and is bounded by, antithetic to, and kinematically linked with, the Clark and Coyote Creek faults (Figs. 3 and 4) (Dibblee, 1954; Bartholomew, 1968, 1970; Theodore and Sharp, 1975; Ryter, 2002; this study). Offset on the Inspiration Point fault is difficult to estimate, but Ryter (2002) suggested <300 m on the basis of potentially correlatable folds. Several NE-plunging folds trend subparallel to the Inspiration Point fault northwest of its trace (Fig. 4) (Dibblee, 1954, 1984; Bartholomew, 1968; Theodore and Sharp, 1975; Ryter, 2002; Lutz, 2005; this study). In places, these folds are unconformably overlain by and gently deform the Fonts Point Sandstone (Fig. 5). In the eastern Borrego Badlands, two broad, WNW-trending synclines deform the Ocotillo Formation (Fig. 4) (Dibblee, 1954, 1984; Bartholomew, 1968; Pettinga, 1991; Ryter, 2002). These kilometer-scale synclines and intervening anticline are subparallel to the Clark fault and reflect active, transpressive, off-fault strain.

OCOTILLO FORMATION IN THE BORREGO BADLANDS

Sedimentary Lithofacies

The Ocotillo Formation in the Borrego Badlands is divided into four main sedimentary lithofacies based on grain size, lithology, and sedimentary structures. These are (1) sandy conglomerate, (2) conglomeratic sandstone, (3) tabular-bedded sandstone and siltstone, and (4) mudstone with siltstone and sandstone. The lithofacies record deposition in diverse terrestrial conditions and environments ranging from alluvial fans to dryland rivers and lake margins.

Sandy Conglomerate (SC)

Sandy conglomerate is exposed only in the northeastern Borrego Badlands (Fig. 4) and consists of moderately sorted clast-supported pebble to pebble-cobble conglomerate interbedded with poorly sorted pebbly sandstone (Fig. 6A). Beds are tabular to broadly lenticular, 20–40 cm thick, ungraded, massive to horizontally stratified, and locally display 10–30 cm of basal erosional relief. Thin discontinuous muddy siltstone laminae commonly cap distinct 10–20 cm thick upward-fining intervals. Segregation of conglomerate from horizontally stratified pebbly

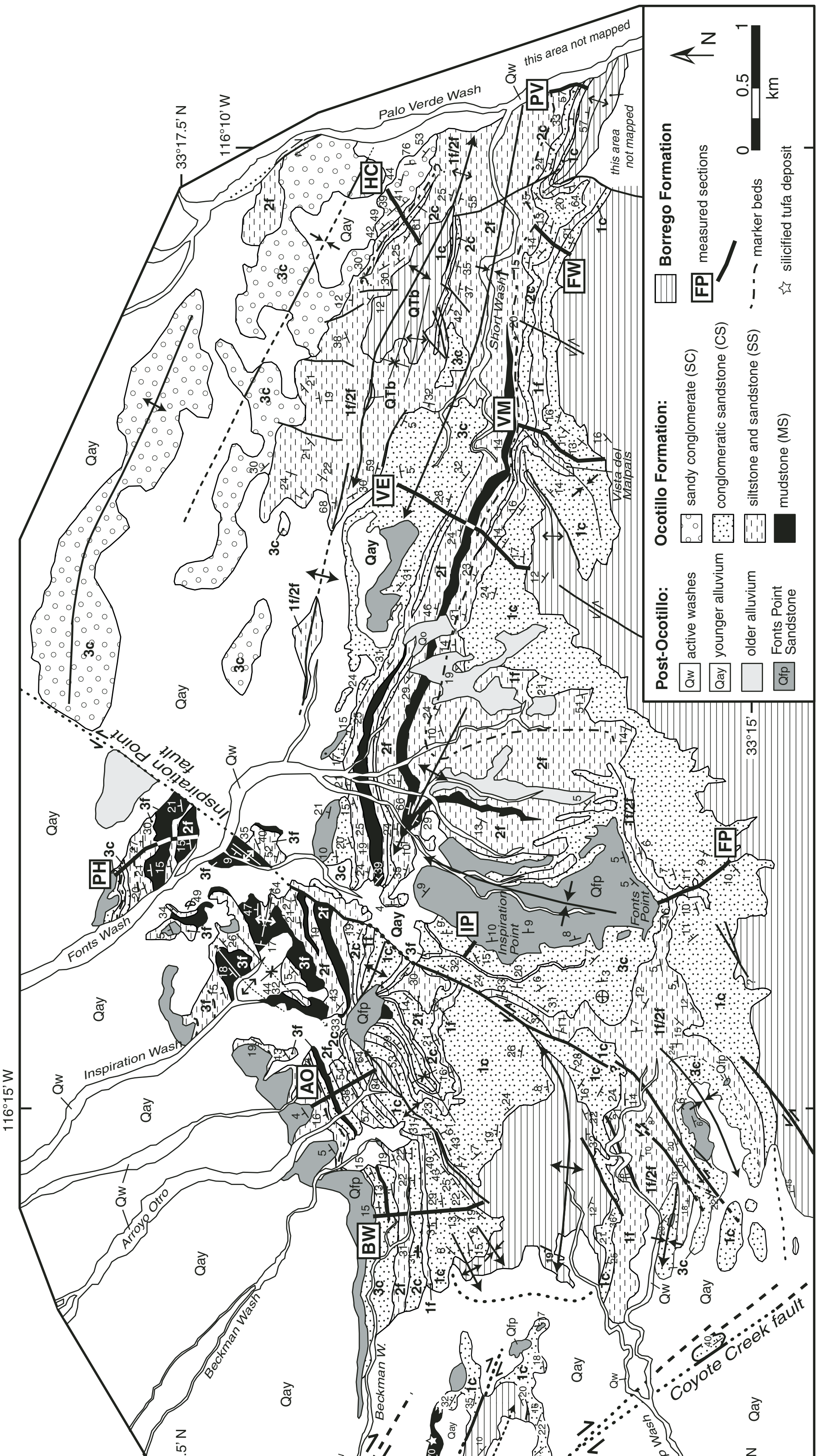

Figure 4. Geologic map of the Borrego Badlands showing lithofacies in the Ocotillo Formation, major structures, and location of measured sections (Fig. 7). Based on detailed (1:12,000 scale) map of Lutz (2005), modified in the west by R. Dorsey. Northeast part of map is modified and interpreted after Bartholomew (1968). Number-letter labels identify Ocotillo members 1–3; c—coarse facies; f—fine facies. See text for further explanation. AO—Arroyo Otro; BW—Beckman Wash; FP—Fonts Point; FW—Fault Wash; HC—Hidden Canyon; IP—Inspiration Point; PH—Painted Hill; PV—Palo Verde Wash; VE—Valle Escondido; VM—Vista del Malpais. SST—sandstone.

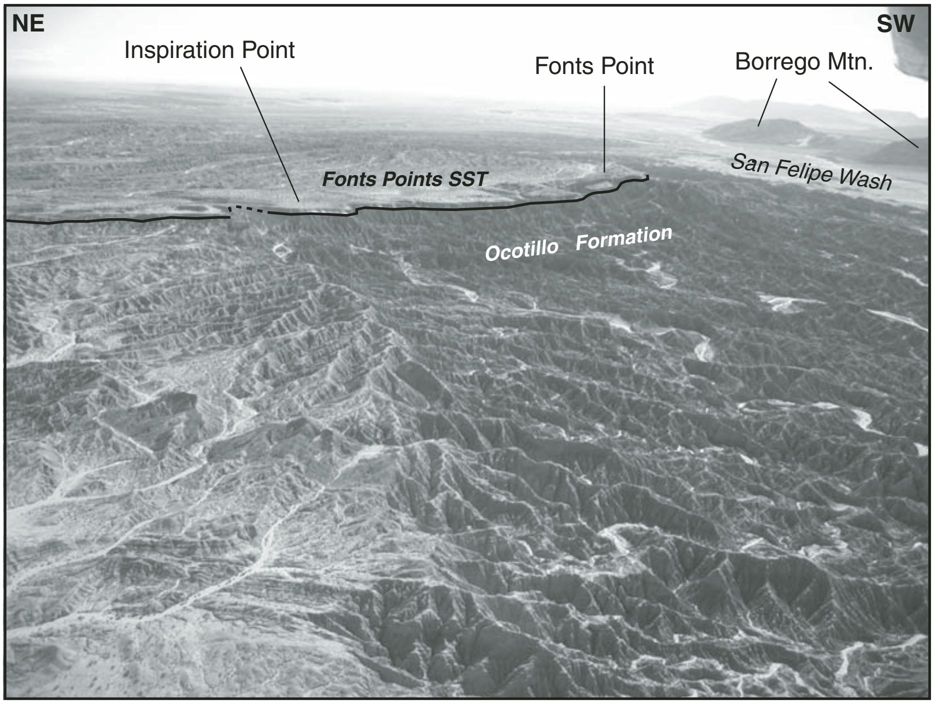

Figure 5. Oblique aerial photograph of the western Borrego Badlands showing the Fonts Point Sandstone, which caps the Ocotillo Formation and marks the top of the erosional escarpment at Fonts Point and Inspiration Point. The Fonts Point Sandstone is gently deformed by a broad NNE-trending fold north of Fonts Point (Fig. 4). View is to the southeast. Photo by R. Dorsey. SST—sandstone.

sandstone, and discrete interbedding of these two lithologies, are typical (Fig. 6A).

This facies is interpreted to record punctuated deposition of gravel and pebbly sand by sheet floods in the medial to proximal part of an alluvial fan system (e.g., Heward, 1978; Rust and Koster, 1984; Wells and Dohrenwend, 1985; Blair, 1987a; Blair and McPherson, 1994). Lack of cross-bedding, and abundant horizontal stratification in interbedded conglomerate and pebbly sandstone, indicate that critical to supercritical flow conditions existed during deposition by sheet floods on an unconfined sloping surface. By analogy with similar facies observed in modern alluvial fan deposits in Colorado (Blair, 1987a), we infer that alternation of clast-supported conglomerate and stratified pebbly sandstone reflects autocyclic fluctuations in flow velocity produced by development and destruction of antidune waves during floods.

Conglomeratic Sandstone (CS)

Conglomeratic sandstone is abundant in the study area and consists of two main variants: pebbly sandstone (coarse variant) and weakly bedded sandstone (fine variant). The coarse variant consists of tabular to low-angle cross-bedded, poorly sorted pebbly sandstone and sandstone with common thin stringers of sandy pebble conglomerate (Fig. 6B). Discontinuous horizontal stratification and low-angle trough cross-bedding are common, and shallow channel scours typically display less than 1–3 cm of erosional relief. Weakly bedded sandstone (fine variant) is characterized by tabular to low-angle trough cross-bedding in fine- to very coarse-grained sandstone with rare thin discontinuous stringers of granule conglomerate and siltstone (Fig. 6C). Weakly graded massive sandstone with indistinct bedding is also common. Weakly developed pedogenic calcite horizons are common in central and western parts of the study area, and well-developed tabular pedogenic carbonate horizons are present but rare.

Conglomeratic sandstone records flashy deposition in a range of subenvironments that formed in an arid piedmont setting (e.g., Miall, 1978; Rust and Koster, 1984; Wells and Dohrenwend, 1985; Collinson, 1996; Blair, 1987b; Blair and McPherson, 1994). The coarse variant (pebbly sandstone) was deposited by shallow streamflows and sheet floods in distal coalesced alluvial fans that passed downstream into an ephemeral braid plain system. Weakly graded massive sandstone with pebble stringers represents shallow channel-fill deposits transported by traction in sheet floods, and cross-bedded sandstone records shallow channel-fill and low-relief longitudinal bar migration. Pedogenic calcite nodules were produced by intermittent soil development in a proximal overbank setting (e.g., Retallack, 2001). Two well-developed, areally extensive ~0.5 m thick carbonate horizons in the western Borrego Badlands record prolonged soil development on abandoned (and later reoccupied) fluvial terrace surfaces.

Bedded Sandstone and Siltstone (SS)

Bedded sandstone and siltstone are exposed in varying abundance in the Borrego Badlands (Fig. 4) and are characterized by thin- to medium-bedded siltstone and fine- to medium-grained sandstone with distinctive, laterally continuous tabular bedding. Ripple and climbing-ripple laminations defined by abundant detrital biotite are common, as are structureless beds of similar grain size with admixed biotite. Thin beds and planar laminae of 100% detrital biotite are also locally common. Thin beds of weakly laminated mudstone and weakly developed horizons of nodular pedogenic carbonate in fine-grained sandstone are also present.

This lithofacies records deposition of distal to proximal crevasse-splay sheet sands in either a proximal fluvial floodplain setting or a fluvial delta at the margin of a shallow lake (e.g., Collinson, 1996; Eberth and Miall, 1991; Buchheim et al., 2000; Michaelsen et al., 2000; Turkmen and Kerey, 2000). The large lateral extent and continuity of individual beds and paucity of strong bioturbation and soil features indicate unconfined deposition with minimal influence of biogenic and pedogenic processes. Biotite laminae in ripple-laminated sandstone beds are attributed to hydraulic sorting by shallow current bed forms, and climbing-ripple-laminated sandstones represent current bed forms and rapid sediment fallout during transport by slightly higher-energy currents.

Mudstone with Siltstone and Sandstone (MS)

This lithofacies is most abundant in the north-central part of the study area and is laterally equivalent to coarser facies to the east, west, and south (Fig. 4). The main lithology is pale reddish to reddish-gray, massive to weakly bedded, weakly laminated mudstone and claystone with laterally continuous tabular bedding. Intercalated in the mudstone facies are very thin (≤1 mm) convoluted laminae of siltstone to very fine-grained sandstone, thin beds of well-sorted very fine-grained ripple-laminated sandstone with detrital biotite, and thin beds of moderately well-sorted ripple cross-laminated sandstone. Thin sandstone beds are commonly associated with sparse, weakly developed, very thin root casts in underlying mudstone. Thin, discontinuous gypsum beds and desiccation cracks are only rarely observed.

Mudstone accumulated by suspension settling of clay and silt in a low-energy marshy floodplain, palustrine, or lake-margin environment. Quiet conditions were punctuated by input of fine sand from fluvial or deltaic distributary channels during river floods (e.g., Collinson, 1996; Eberth and Miall, 1991; Buchheim et al., 2000; Michaelsen et al., 2000; Turkmen and Kerey, 2000). Convoluted laminae record disturbance of unconsolidated sediment by floods or earthquakes. The paucity of gypsum layers, mud cracks, soil horizons, and other desiccation features indicates that complete subaerial exposure was rare. Cross-bedded sandstone and associated weakly developed pedogenic carbonate horizons record brief episodes of crevasse-splay sheet-sand deposition and accompanying plant colonization in a wet marshy environment.

Physical Stratigraphy and Basin Architecture

Physical stratigraphy and basin architecture were documented in this study to determine the timing and nature of basin response to regional tectonic activity and slip on basin-bounding faults. This was accomplished through detailed measuring and description of ten stratigraphic sections (Fig. 7), geologic and facies mapping (Fig. 4), and construction of basin-scale facies panels (Fig. 8) and isopach maps (Fig. 9). We define three informal stratigraphic members in the Ocotillo Formation, members 1, 2, and 3, based on their stratigraphic position, lithofacies associations, and correlation through detailed (1:12,000 scale) geologic mapping. Each member is further subdivided into a coarse-grained submember, c, that includes conglomeratic sandstone (CS) and sandy conglomerate (SC) lithofacies, and a fine-grained submember, f, consisting of bedded sandstone and siltstone (SS) and mudstone (MS) lithofacies. Thus the finest level of stratigraphic subdivision is represented by submembers 1c, 1f, 2c, 2f, 3c, and 3f (Figs. 4, 7, and 8).

To construct the facies panels in Figure 8, measured sections were hung from the base of the Fonts Point Sandstone. One problem with this datum is that its basal contact with the Ocotillo Formation changes from conformable in sections southeast of the Inspiration Point fault to an angular unconformity northwest of the Inspiration Point fault, with clear NE-ward tilting and SW-ward truncation of units. However, the Fonts Point Sandstone is the best available datum for reconstructing basin geometry because it is a widespread sheetlike deposit that records a short period of post-Ocotillo alluvial deposition. Use of this marker thus provides information about thickness variations in units that were not affected by pre–Fonts Point erosion, and it reveals the overall basin geometry prior to Fonts Point deposition.

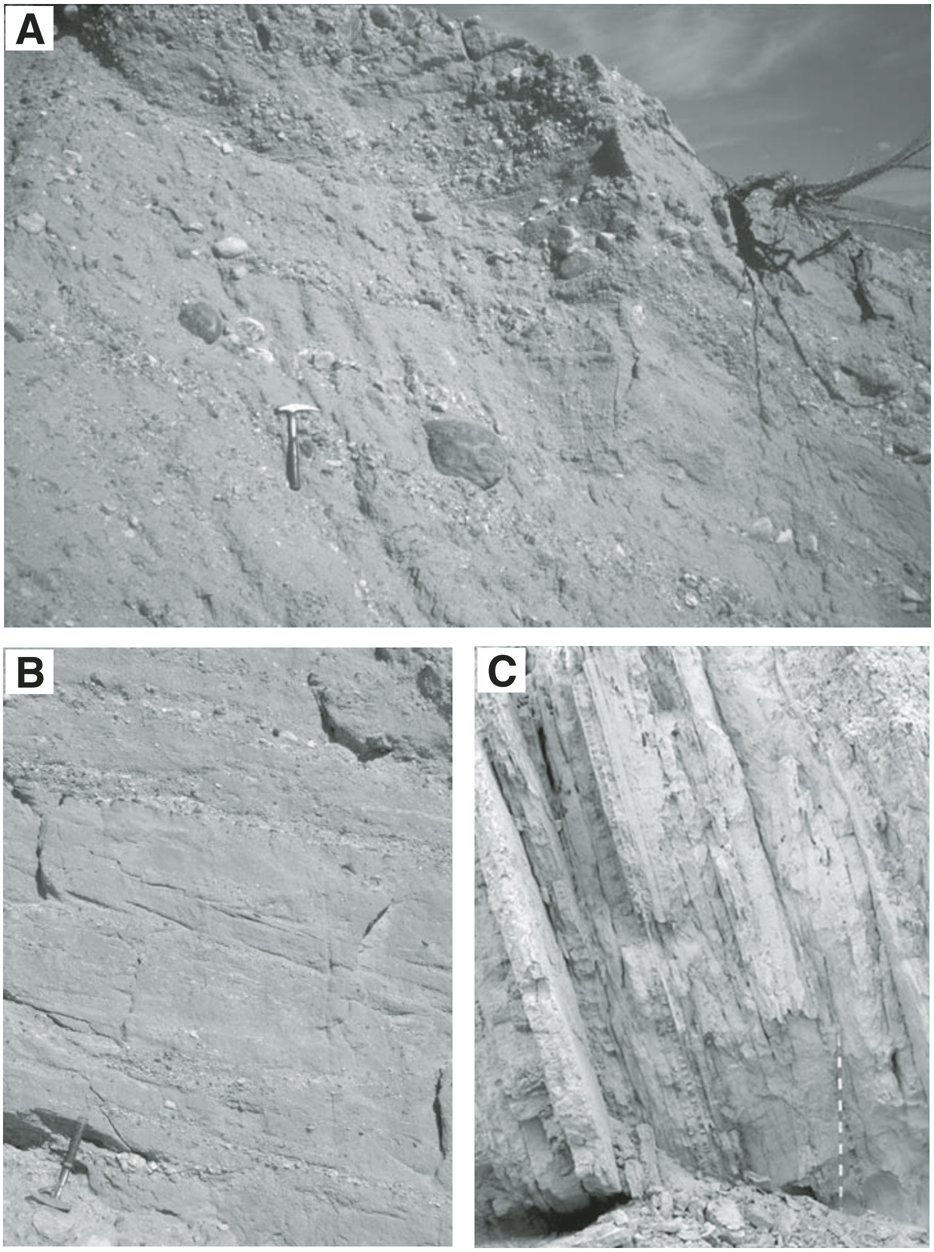

Figure 6. Photographs of lithofacies in the Ocotillo Formation. (A) Sandy conglomerate with gravel-sand couplets. Hammer is 33 cm long. (B) Conglomeratic sandstone (CS), coarse variant. Hammer is 33 cm long. (C) Bedded sandstone and siltstone lithofacies (SS) with planar tabular bedding. Divisions in measuring staff are 10 cm long.

The basal contact of the Ocotillo Formation displays significant lateral variation. In the west at Beckman Wash (BW), lacustrine claystone at the top of the Borrego Formation contains a moderately developed arid-climate paleosol with dispersed small calcite nodules, red and green mottling, weakly developed columnar peds, and sand-filled desiccation cracks up to ~1 m deep. The paleosol is abruptly overlain by conglomeratic sandstone of the basal Ocotillo Formation (Fig. 7). Detailed facies mapping reveals that the uppermost 3–5 m of Borrego Formation claystone and siltstone in this area are laterally continuous and are not eroded along the basal Ocotillo contact. The contact at Beckman Wash

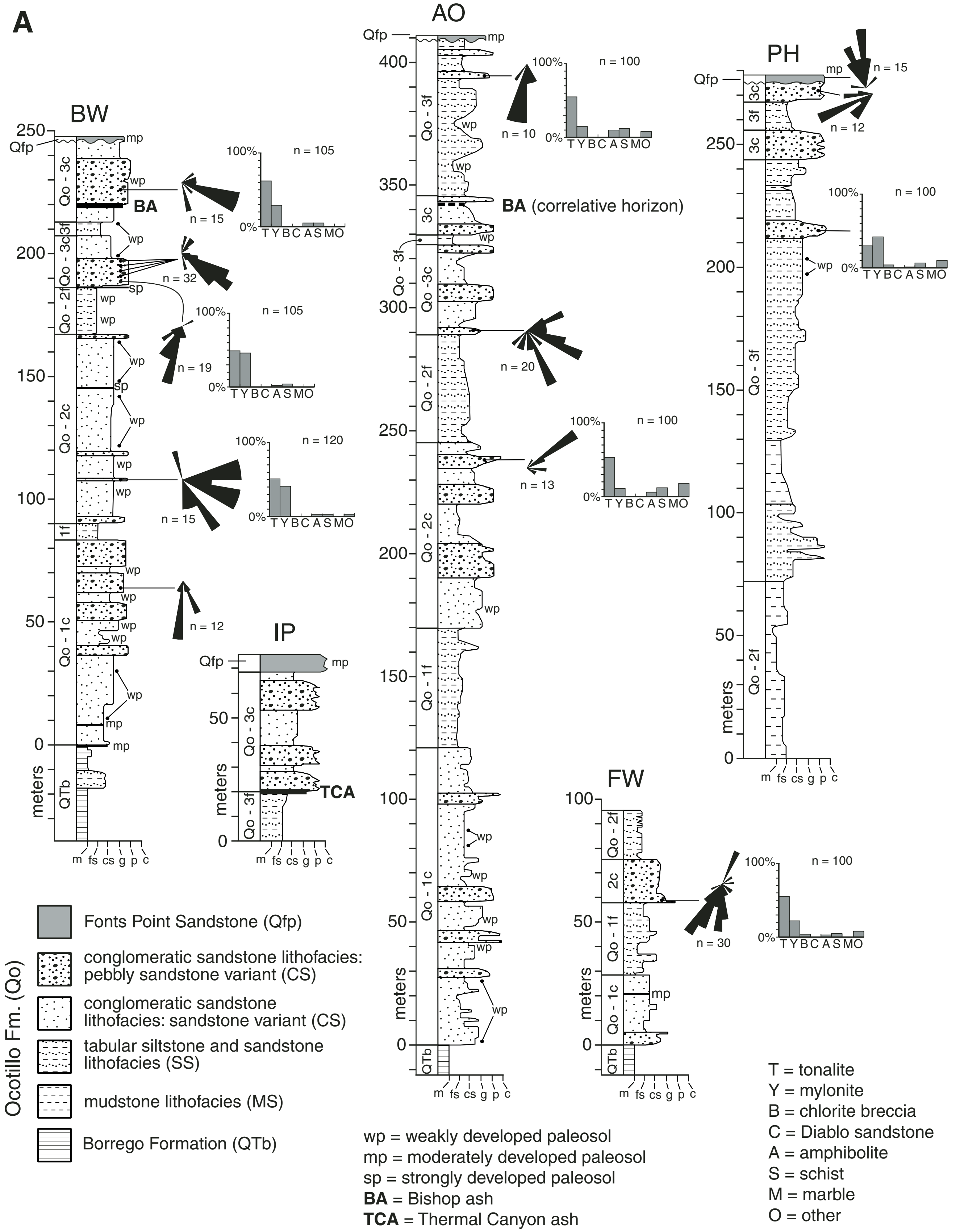

Figure 7 (*on this and following page*). Measured stratigraphic sections with paleocurrent directions and clast count data. Location of sections shown in Figure 4. See text for discussion. m—mud; fs—fine sand; cs—coarse sand; g—granule; p—pebble; c—cobble.

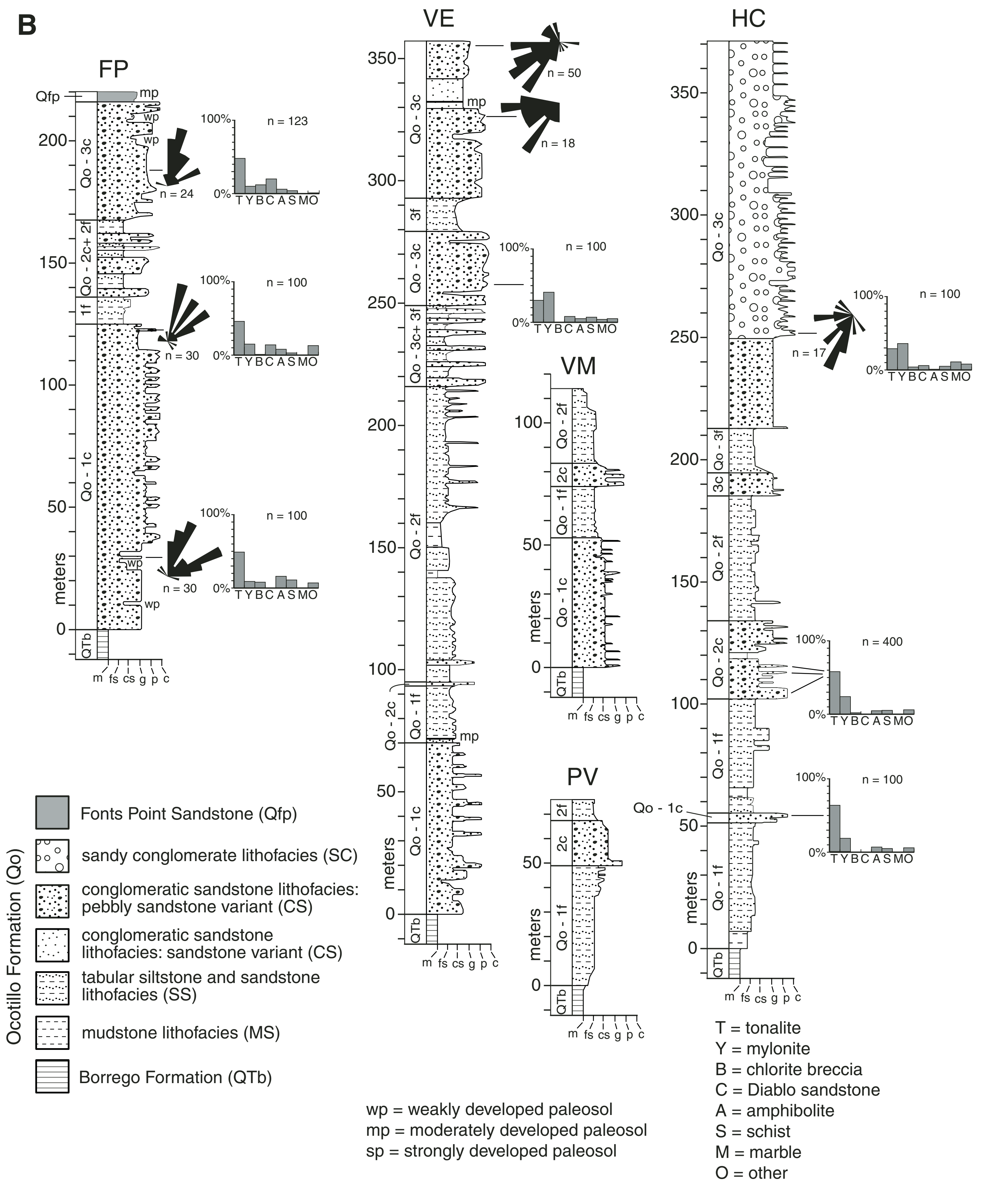
B
FP
VE
HC
VM
PV
Qfp
mp
wp
Qo - 3c
Qo - 2c+ 2f
1f
Qo - 1c
QTb
meters
n = 123
n = 24
n = 100
n = 30
100%
0%
T Y B C A S M O
m fs cs g p c
Qo - 3f
Qo - 3c+ 3f
Qo - 2f
Qo - 2c
Qo - 1f
n = 50
n = 18
n = 17
n = 400
Fonts Point Sandstone (Qfp)
Ocotillo Formation (Qo)
sandy conglomerate lithofacies (SC)
conglomeratic sandstone lithofacies: pebbly sandstone variant (CS)
conglomeratic sandstone lithofacies: sandstone variant (CS)
tabular siltstone and sandstone lithofacies (SS)
mudstone lithofacies (MS)
Borrego Formation (QTb)
wp = weakly developed paleosol
mp = moderately developed paleosol
sp = strongly developed paleosol
T = tonalite
Y = mylonite
B = chlorite breccia
C = Diablo sandstone
A = amphibolite
S = schist
M = marble
O = other

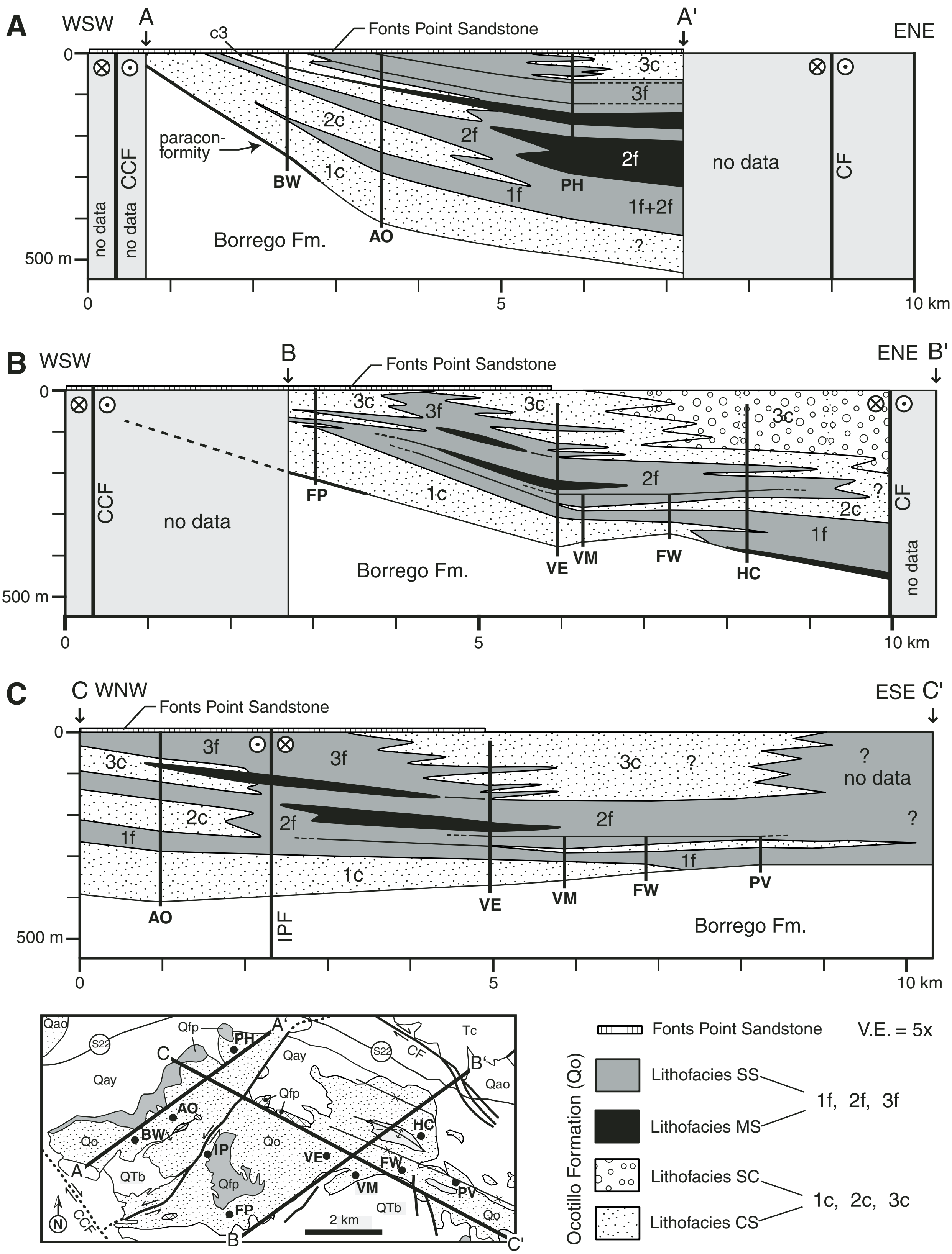

Figure 8. Facies panels showing architecture of the Ocotillo Formation immediately following deposition of the Fonts Point Sandstone. Measured sections shown in Figure 7. Vertical exaggeration in all panels is 5×. CCF—Coyote Creek fault; CF—Clark fault; IPF—Inspiration Point fault; lithofacies CS—conglomeratic sandstone; lithofacies MS—mudstone with siltstone and sandstone; lithofacies SC—sandy conglomerate; lithofacies SS—bedded sandstone and siltstone.

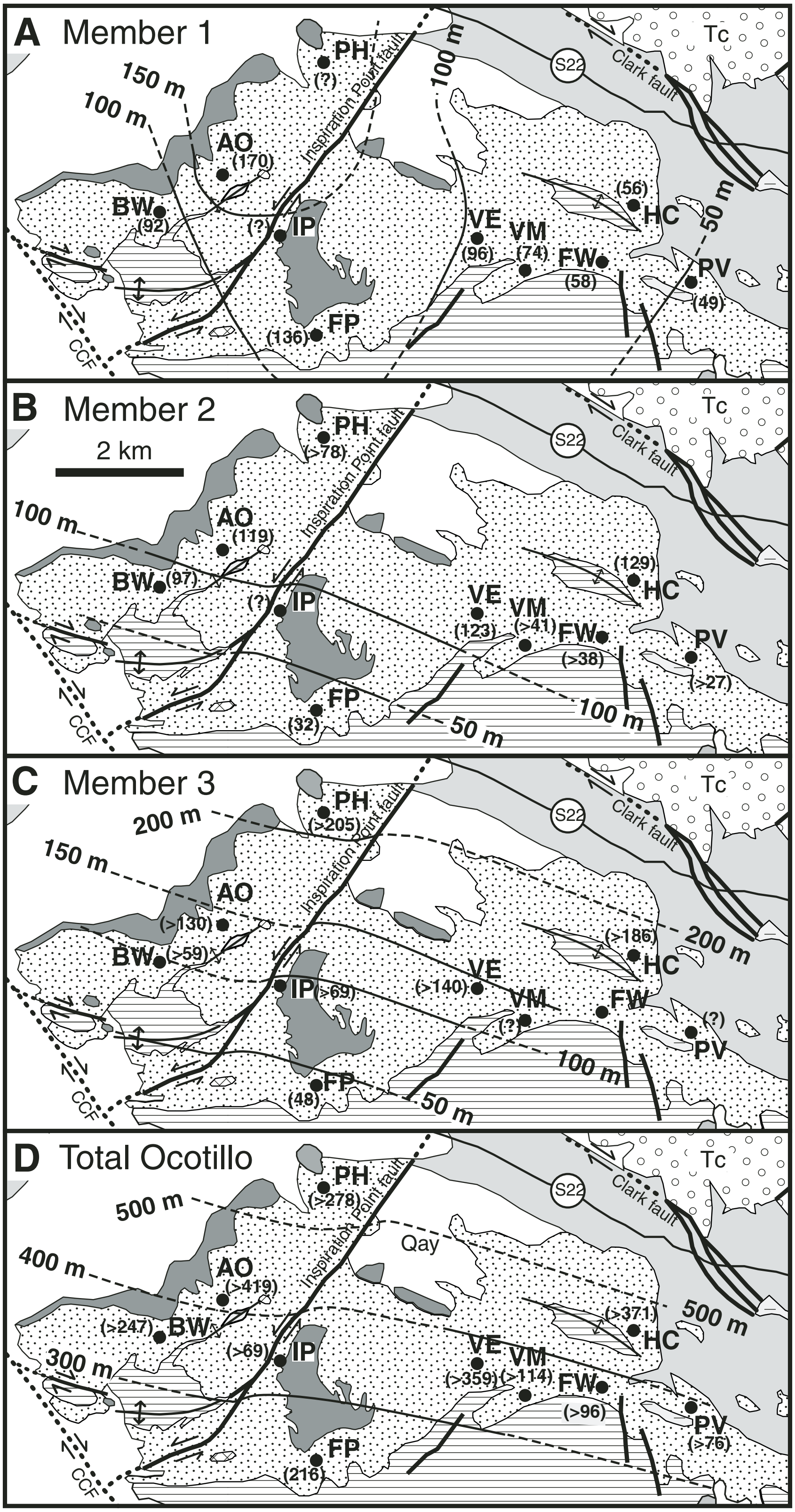

Figure 9. Isopach maps of the Ocotillo Formation in the Borrego Badlands based on thicknesses obtained from measured sections (Fig. 7). (A) Ocotillo member 1. (B) Ocotillo member 2. (C) Ocotillo member 3. (D) Total Ocotillo Formation. CCF—Coyote Creek fault.

is thus interpreted to be a short-lived depositional hiatus, or paraconformity, that formed by temporary desiccation of the Borrego Lake bed prior to the abrupt change to deposition of coarse pebbly alluvium in a distal alluvial fan setting. In central sections (Figs. 4 and 7), upper Borrego Formation claystone is overlain by basal Ocotillo Formation sandstone and pebbly sandstone along a sharp but conformable contact that shows no evidence for erosional truncation or soil formation beneath the contact. At the two northeasternmost locations (HC, PV), uppermost Borrego Formation claystone is conformably and abruptly overlain by bedded sandstone and siltstone (SS) and mudstone (MS) lithofacies of the basal Ocotillo Formation. East of Palo Verde Wash, the lower member passes laterally into lacustrine claystone and siltstone lithologically identical to the Borrego Formation.

The Ocotillo Formation displays overall lateral coarsening toward basin margins, fining into the basin center, and NNE-ward thickening obliquely toward the Clark fault (Fig. 8). Total preserved thickness varies between ~300 and 500 m in the study area. Facies panels reveal thickening of members 2 and 3 toward the north-northeast across the basin, with angular truncation of tilted Ocotillo Formation in the southwest (Fig. 8). The abundance of paleosols covaries systematically with thickness trends across the basin (Fig. 7). Paleosols are most abundant in the southwest at Beckman Wash (BW); they become less abundant in central locations (AO, FP, VE); and they are absent in the northeast where the section is the thickest (VM, PV, HC) (Fig. 4). This spatial variation in paleosol abundance is similar to that observed in Pliocene-Pleistocene deposits of the Rio Grande rift, where paleosols are best developed in areas of slow sedimentation in the hanging wall of half-graben basins (Mack and Seager, 1990).

Paleocurrents

Paleocurrent data were collected primarily from measurements of clast imbrication planes in pebbly sandstone and sandy conglomerate, and locally include cross-bedding and channel axis orientations. Corrections for bedding dip steeper than 10° were made using stereographic software. No corrections were made for rotation about a vertical axis because there is no evidence for significant basin rotation (Housen et al., 2004; this study).

Paleocurrent indicators in the western Borrego Badlands (BW and AO) record dominantly SE- to S-directed sediment transport, with minor transport toward the northeast (Fig. 7). In the south-central part of the area (FP section), transport was consistently toward the north and northeast. In contrast, eastern parts of the study area (HC, VE, FW) record consistent SW-directed paleotransport. Paleocurrents in the upper part of the PH section (north-central) change abruptly from southwest directed in the upper Ocotillo Formation to overall north to northwest directed in the Fonts Point Sandstone (Fig. 7).

Conglomerate Clast Compositions

Clast counts were conducted in pebble and cobble conglomerate beds to determine the composition of clasts and source areas. Sample populations of 100 or more were collected to ensure statistical significance. Clasts were identified as one of seven categories: tonalite (T), mylonite (Y), chlorite breccia (B), Colorado River–derived sandstone of the Diablo Formation (C), amphibolite (A), schist (S), and marble (M) (Fig. 7). Clasts not fitting into one of these seven categories were classified as "other" (O) and include vein quartz, fine-grained crystalline rock, and unknown or unidentified lithologies. Tonalite, mylonite, chlorite breccia, and metamorphic rocks are common constituents of nearby basement rocks (Dibblee, 1954, 1996; Jahns, 1954; Sharp, 1967; Bartholomew, 1968; Gastil, 1975; Theodore and Sharp, 1975; Calzia et al., 1988). Diablo Formation sandstone is exposed in the southern Santa Rosa Mountains, the southern Borrego Badlands, and northwest of Borrego Mountain (Fig. 3).

Conglomerate clasts in the west (BW, AO, FP; Fig. 7) are dominated by tonalite with minor mylonite, amphibolite, and other clast types. The FP section reveals an up-section increase in reworked Diablo Formation sandstone. Eastern (HC, VE, FW) and north-central (PH) sections generally contain higher percentages of mylonite and marble (Fig. 7), and reworked Diablo Formation sandstone clasts are common in small amounts. The HC section reveals an up-section increase in mylonite and marble and appearance of minor Diablo Formation sandstone.

Magnetostratigraphy

Methods and Data Quality

A magnetostratigraphic study of the Beckman Wash section was conducted to determine the age of the Ocotillo Formation and Fonts Point Sandstone. Oriented samples were collected from 14 sites in the BW measured section Table DR1[1], and each site yielded 3–11 samples. Samples from sites 03Qo8 and 03Qo9 were recovered using 2.5 cm^3 plastic cubes; all other samples were recovered using a water-cooled gasoline-powered diamond core drill. All laboratory measurements were conducted at the Western Washington University Paleomagnetism Lab. Stepwise thermal or alternating-field demagnetization revealed two components of magnetization: The first-removed component was generally isolated between 25 and 40 mT in alternating-field-demagnetized specimens (Fig. 10A) and 160–360 °C in thermally demagnetized specimens (Figs. 10B and 10C). The second-removed component was generally isolated above 40 mT in alternating field demagnetized specimens (Fig. 10A) and 400 °C in thermally demagnetized specimens (Figs. 10B and 10C). The second-removed components typically have well-defined vectors, as shown on orthogonal plots that approach or converge to the origin (Fig. 10).

Four grades of data quality were recognized. Type I data resulted in well-defined vector components with a maximum angular deviation (MAD) of <8° (Fig. 10). Type II data produced moderately well-defined vector components with a MAD greater than 8° but less than 15°. Type III data had no definable vector components with a MAD of less than 15° but allowed for qualitative evaluation of normal or reversed polarity: Some sites interpreted as reversed polarity track along a great circle toward the reversed field direction. Magnetization paths of type IV data were very poorly defined and exhibited no relevant quantitative or qualitative results.

Statistical analysis of site means averaged type I and II data for each site (Table DR2). Eight sites have mean directions that are well clustered (defined here as $k > 15$), and were used to calculate mean directions in both in situ and tilt-corrected coordinates (Table DR2). The similarities in bedding attitude for these sites resulted in an inconclusive paleomagnetic fold test, but the precision parameter (k) was observed to increase from $k = 38$ in in situ coordinates to a maximum value of $k = 48$ in 100% tilt-corrected coordinates. The 100% tilt-corrected mean (Declination [D] = 0.4°, Inclination [I] = 38.2°, $k = 48$, $\alpha_{95} = 8.1°$, $N = 8$, k and α_{95} are Fisher statistics for mean directions) indicates that little or no significant rotation has occurred at this site during the past 1.1 m.y.

Age of the Ocotillo Formation

Absolute age control for the Ocotillo Formation in the western Borrego Badlands is provided by the 0.76 Ma Bishop ash 220 m above the base of the Ocotillo Formation (Fig. 11) (Remeika and Beske-Diehl, 1996; Sarna-Wojcicki et al., 2000) and the 0.74 Ma Thermal Canyon ash high in the section near Inspiration Point

[1]GSA Data Repository item 2006217, Tables DR1 and DR2, is available on the Web at http://www.geosociety.org/pubs/ft2006.htm. Requests may also be sent to editing@geosociety.org.

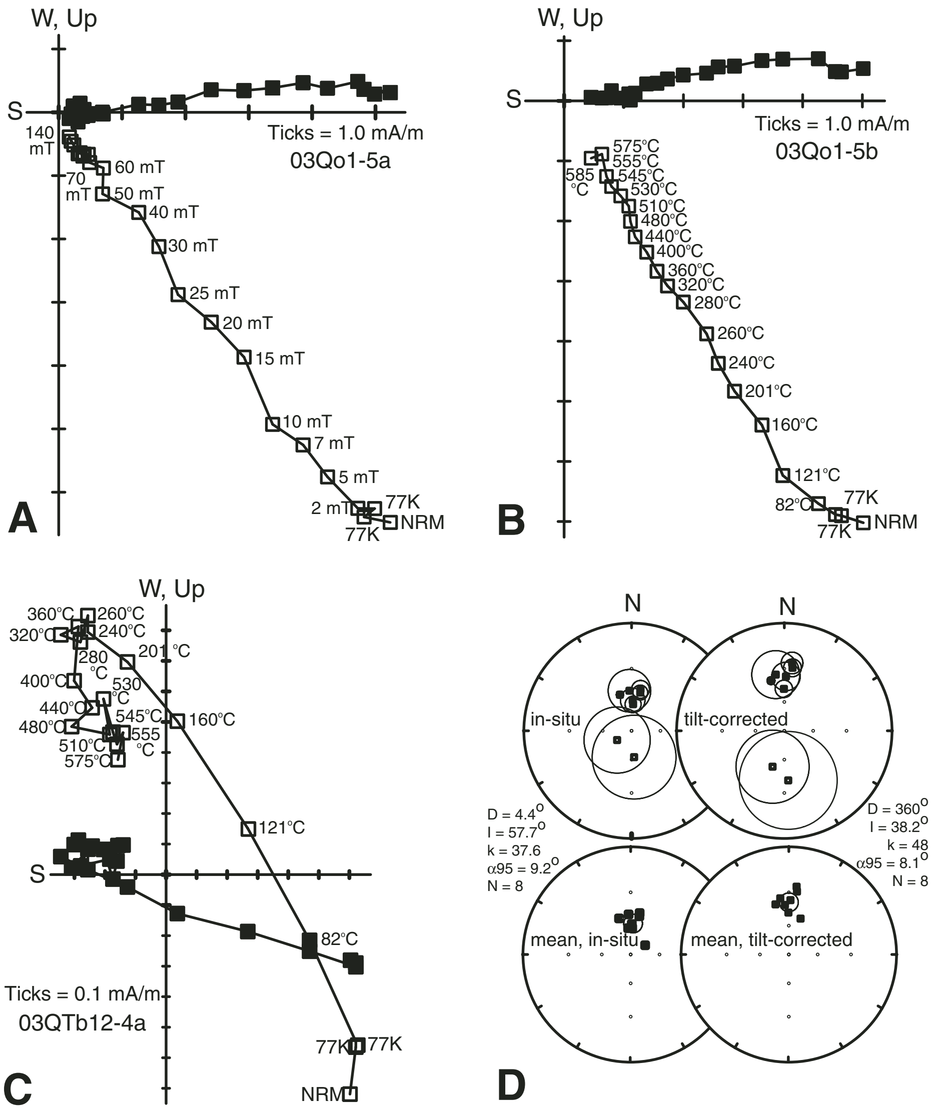

Figure 10. Paleomagnetic data and results. A–C are Zijderveld plots showing demagnetization behavior for type I data. (A) Normal polarity, alternating-field demagnetization. (B) Normal polarity, thermal demagnetization. (C) Reversed polarity, thermal demagnetization. (D) In situ and tilt-corrected site means from paleomagnetic analysis. The expected values for this location are D = 360°, I = 52.7°. Geomagnetic polarity time scale from Cande and Kent (1995). NRM—natural remanent magnetism; D—declination; I—inclination; k and α_{95} are Fisher statistics for mean directions; 77K—77 degrees kelvin.

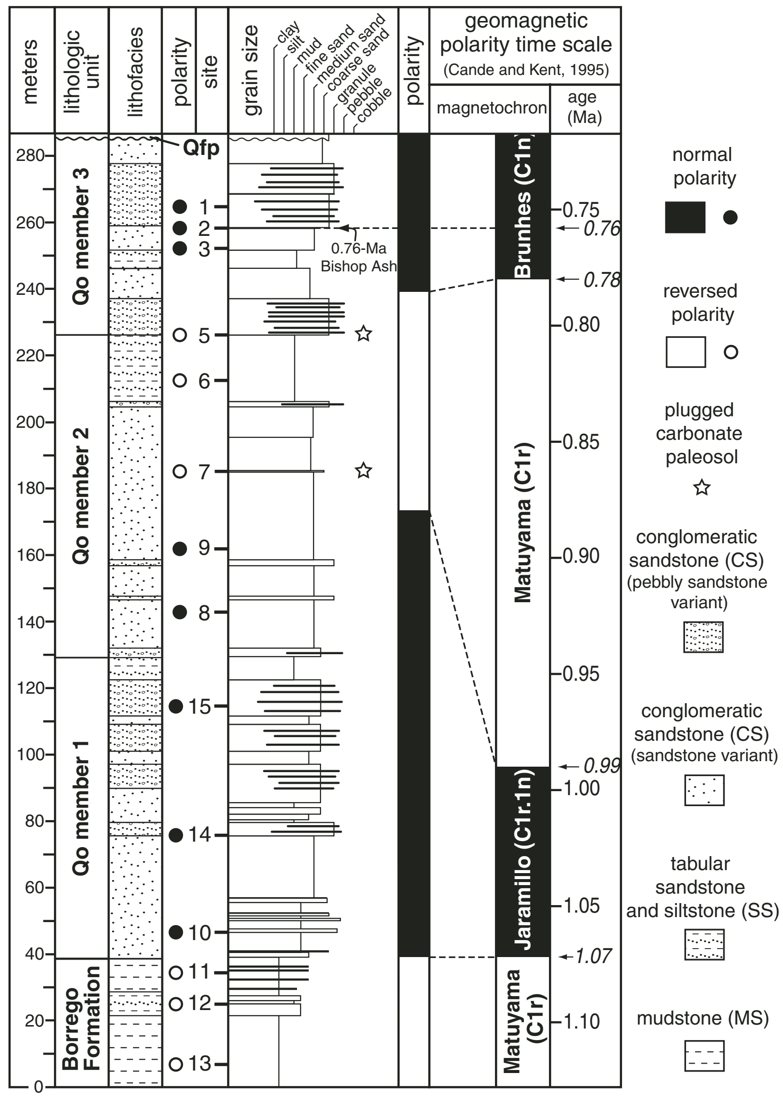

Figure 11. Beckman Wash measured section showing thickness, lithofacies, paleomagnetic sampling positions, and correlation to the geomagnetic polarity time scale (Cande and Kent, 1995). The lower reversal is interpreted to coincide with the Borrego-Ocotillo contact. The upper two reversals are placed an equal distance between sites of opposite polarity. Qo—Ocotillo Formation; Qfp—Fonts Point Sandstone.

(Fig. 7) (Sarna-Wojcicki et al., 1997; Remeika, 2006). The common occurrence of *Mammuthus imperator* fossils in the basal 200 m of the Ocotillo Formation restricts the age of the Ocotillo to less than 1.5 Ma (Remeika and Jefferson, 1993; Jefferson and Remeika, 1994; Bell et al., 2004; Remeika, 2006). Other age-diagnostic vertebrate fossils in the Ocotillo Formation include *Equus bautistensis* and *Camelops huerfanensis*, confirming a middle to late Pleistocene age (Remeika, 1998; Jefferson, 2001).

Three polarity reversals are identified in the BW section (Fig. 11; Table DR2). The lowest polarity change is reversed-to-normal and occurs at the contact between the Borrego and Ocotillo Formations. Based on independent age controls summarized above, we interpret this reversal to be the boundary between the reverse-polarity Matuyama Magnetochron and the normal-polarity Jaramillo Subchron (1.07 Ma) (Cande and Kent, 1995; Singer and Brown, 2002). Because the polarity reversal coincides with a major lithologic contact, the presence of an unconformity or depositional hiatus is suggested. We assume that the reversal occurred sometime during (or at the beginning or end of) formation of the moderately developed Aridisol below the Borrego-Ocotillo contact. The time represented by this hiatus is probably ~10–50 k.y. (e.g., Gile et al., 1981; Birkeland, 1999; Retallack, 2001). Lateral persistence of the paleosol and upper 5 m of Borrego Formation over distances of up to 3 km in this area indicates that the contact represents a short-lived nondepositional hiatus (paraconformity) that did not involve erosion of sediments from the upper Borrego Formation. Based on these constraints, the age of the oldest Ocotillo sediment at Beckman Wash is bracketed between 1.07 and 1.02 Ma, or 1.045 ± 0.025 Ma, which we round to 1.05 ± 0.03 Ma. The second polarity change, at 174 ± 12 m, is correlated to the transition from the Jaramillo Subchron to the upper reversed part of the Matuyama Magnetochron (0.99 Ma; Fig. 11) (Cande and Kent, 1995; Horng et al., 2002). The highest polarity change (239 ± 13 m) is ~18 m below the Bishop ash and records the transition from the Matuyama to the Brunhes Magnetochron (0.78 Ma).

Sedimentation Rates

Measured thicknesses and age determinations permit calculation of sediment accumulation rates in the Ocotillo Formation (Fig. 11; Table 1). Calculated errors consider the thickness between sampling sites and unknown duration and exact age of the paleosol at the Borrego-Ocotillo contact. The average sedimentation rate for the whole Ocotillo Formation at Beckman Wash is 0.68–0.86 mm/yr (Table 1). Isolating different time intervals, we estimate faster sedimentation rates in the lower Ocotillo Formation (~1.4–3.9 mm/yr) and slower rates (~0.2–1.6 mm/yr) in the upper part of the section. The large error in the lower half of the section is due to uncertainty in the length of time represented by the paleosol at the top of the Borrego Formation (~10–50 k.y.; Gile et al., 1981). The most precise rate estimate for the upper half of the section is obtained from the interval between the top of the Jaramillo Subchron (0.99 Ma) and the Bishop ash (0.76 Ma), which yields a sedimentation rate of 0.32–0.42 mm/yr (Fig. 11; Table 1). This rate is used for estimating the age of the Fonts Point Sandstone (below).

Test of Basin Rotation

The results of this study indicate rotation of 0° ± 8°, relative to the expected dipole field direction, indicating that less than 8° of rotation has occurred with 95% confidence (Fig. 10; Table DR2). Abstracts describing prior paleomagnetic studies reported ~30° of clockwise rotation in the past 0.7 m.y. in the western Borrego Badlands (Bogen and Seeber, 1986). Later abstracts refined this interpretation to 21° ± 7° of synbasinal clockwise rotation at Arroyo Otro (Scheuing and Seeber, 1991; Scheuing et al., 1991). Because no major structures exist between Beckman Wash and Arroyo Otro, it is unlikely that the two locations experienced significantly different rotation histories. Data from the previous unpublished studies are not available, so we cannot assess the origin of this discrepancy. We therefore conclude that there has been less than ~8° of vertical-axis rotation in the western Borrego Badlands during the past ~1.0 m.y.

FONTS POINT SANDSTONE

The Fonts Point Sandstone is an ~2 to 8 m thick unit of well-cemented, laterally extensive conglomeratic sandstone that overlies the Ocotillo Formation in the Borrego Badlands (Figs. 4, 5, 7, and 8) (Remeika and Pettinga, 1991; Ryter, 2002; this study). It is a thin, sheetlike mesa-capping unit that contains up to four 60 cm thick Aridisols with pedogenic calcite nodules and pervasive desiccation fissures filled with carbonate-cemented sand (Ryter, 2002). The Fonts Point Sandstone is the oldest and most laterally extensive pediment-capping unit in this area, and it provides a useful record of the end of alluvial deposition and transition from basin subsidence to the modern phase of uplift (inversion), deformation, and erosion.

The basal contact of the Fonts Point Sandstone with the underlying Ocotillo Formation is concordant and conformable within a 1 to 2 km wide belt southeast of the Inspiration Point fault, north and west of Fonts Point. Everywhere else, including all locations northwest of the Inspiration Point fault and south of Fonts Point, the contact is an angular unconformity (Figs. 3, 4, 12, and 13). In the western Borrego Badlands northwest of the Inspiration Point fault, tight to open folds in the Ocotillo Formation are overlapped

TABLE 1. CALCULATION OF SEDIMENT ACCUMULATION RATES

Stratigraphic interval	Time interval (Ma)	Duration of time (k.y.)	Minimum interval thickness (m)	Maximum interval thickness (m)	Minimum sedimentation rate (mm yr^{-1})	Maximum sedimentation rate (mm yr^{-1})
From Bishop ash to base of Brunhes	0.76–0.78	20	6	32	0.30	1.60
From Bishop ash to top of Jaramillo	0.76–0.99	230	73	96	0.32	0.42
From Bishop ash to base of Jaramillo	0.76–1.07	310	211.5	223.5	0.68	0.86†
From base of Brunhes to top of Jaramillo	0.78–0.99	210	41	90	0.20	0.43
From base of Brunhes to base of Jaramillo	0.78–1.07	290	179.5	217.5	0.62	0.91†
From top of Jaramillo to base of Jaramillo	0.99–1.07	80	115.5	150.5	1.44	3.90

†Assumes a maximum depositional hiatus of 50 k.y. at the Borrego-Ocotillo contact.

unconformably by the Fonts Point Sandstone, which in turn is gently warped about the same folds (Figs. 4, 5, and 13). South of Fonts Point, the Fonts Point Sandstone is preserved in an erosional remnant where it overlies moderately to steeply dipping beds of the Palm Spring Group on both sides of the Coyote Creek fault (Fig. 3). Here, the Fonts Point Sandstone shows ~10 m of NE-side-up vertical offset on the fault; the amount of strike-slip offset is impossible to measure due to young erosion at the edges of this deposit. Southwest of the Coyote Creek fault, the Fonts Point Sandstone overlies folded and faulted deposits of the Palm Spring Group, West Butte Conglomerate, and a small area of Cretaceous tonalite near the core of the San Felipe anticline at Borrego Mountain (Fig. 3).

We can estimate the age of the conformable base of the Fonts Point Sandstone at Inspiration Point using tephrochronology, sedimentary thickness, and accumulation rates. The section at Inspiration Point includes a tephra that has been chemically correlated to the 0.74 Ma Thermal Canyon ash (Sarna-Wojcicki et al., 1997; Remeika, 2006) in sedimentary lithofacies equivalent to those nearby at Beckman Wash (Figs. 7 and 14). Ocotillo member 3 in the IP and BW sections has a similar thickness (Fig. 9) and thus experienced similar rates of deposition in the two areas. Application of the minimum and maximum sedimentation rates determined at Beckman Wash (0.2–3.9 mm/yr) to the thickness of the Ocotillo Formation above the Thermal Canyon ash at Inspiration Point (49 m) yields a bracketed age of 0.50–0.73 Ma for the base of the Fonts Point Sandstone (Table 1). Because the Thermal Canyon ash is in the upper Ocotillo Formation, we can refine this estimate using a sedimentation rate calculated for the upper Ocotillo Formation at Beckman Wash (0.32–0.42 mm/yr). This rate yields an age of 0.59–0.62 Ma, or 0.60 ± 0.02 Ma, for the conformable base of the Fonts Point Sandstone at Inspiration Point.

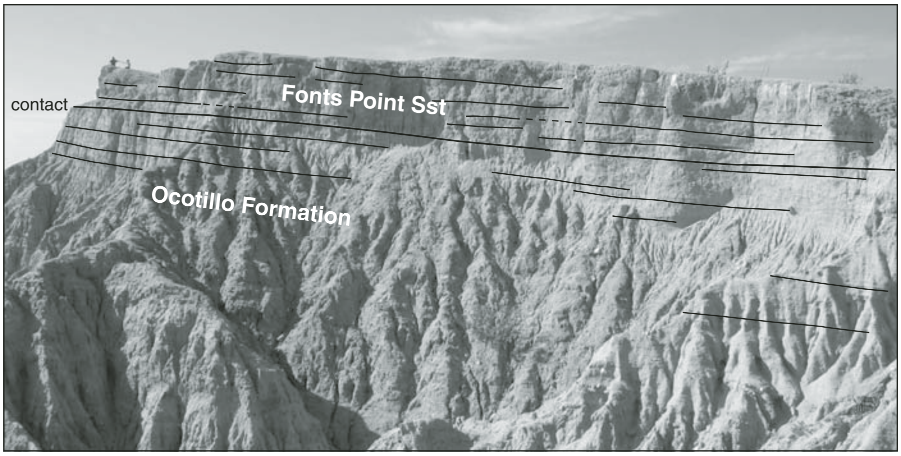

Figure 12. Photograph of exposure at Fonts Point showing example of the conformable contact between the Ocotillo Formation and Fonts Point Sandstone. Thickness of Fonts Point Sandstone is ~3 m at this location. View is toward the southwest. SST—sandstone.

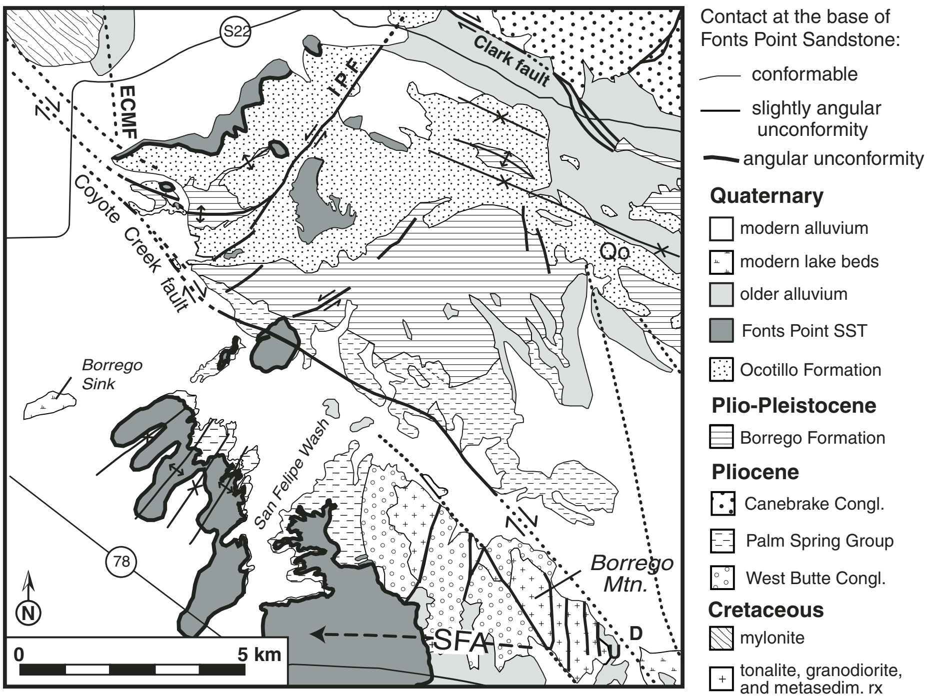

Figure 13. Subcrop map showing change in character of the Fonts Point–Ocotillo contact from a conformable contact at Fonts Point (thin line) to an angular unconformity (thick line) northwest across the Inspiration Point fault (IPF) and south to the San Felipe Wash area. ECMF—East Coyote Mountain fault; CF—Clark fault; SFA—San Felipe anticline; metasedim. rx—metasedimentary rocks; SST—sandstone.

PALEOGEOGRAPHY AND BASIN EVOLUTION

The data presented above record four stages of Pleistocene basin evolution corresponding to deposition of the lower, middle, and upper members of the Ocotillo Formation and the Fonts Point Sandstone (Fig. 15). The age of the different Ocotillo members is determined by basin-scale facies mapping, tracing of marker beds, and correlation to the magnetically dated Beckman Wash section (Fig. 11). Despite the uncertainty introduced by lateral facies changes in the area, the regionally synchronous age of the basal Ocotillo contact (1.05–1.07 Ma) is well known from correlation to other dated sections in the western Salton Trough (Brown et al., 1991; Kirby, 2005). The thin sheetlike Fonts Point Sandstone shows no interbedding or interfingering with Ocotillo deposits and therefore provides a short-lived marker unit that postdates the Ocotillo Formation. Thus the entire Ocotillo Formation represents ~0.5 m.y. of time, and the ages of basin development discussed below are well constrained with data presented above. Shortly

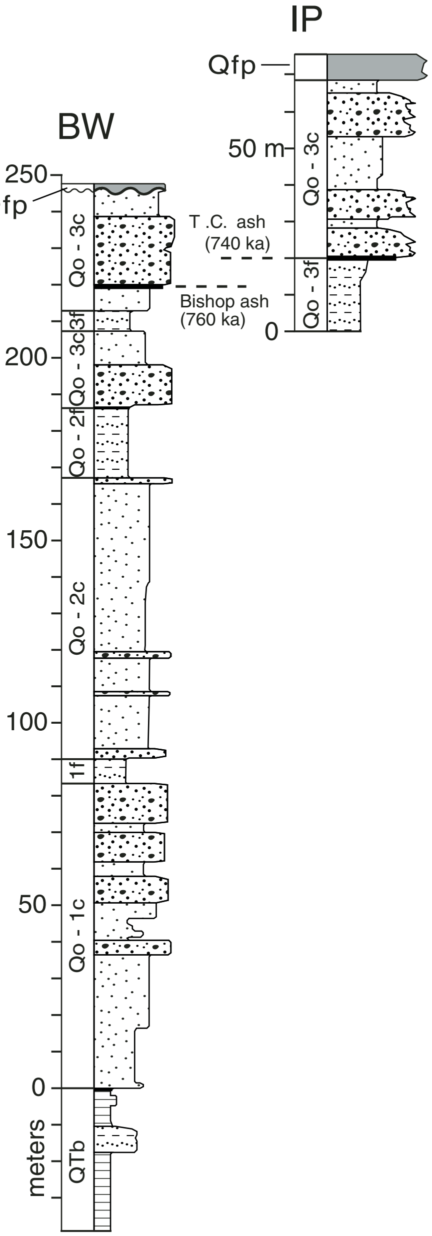

Figure 14. Correlation of the Beckman Wash (BW) section to the Inspiration Point (IP) section. Dashed lines indicate inferred correlation of ash layers between the sections. Ashes in both sections have been identified with trace element geochemistry (Remeika and Beske-Diehl, 1996; Sarna-Wojcicki et al., 1997, 2000; Remeika, 2006).

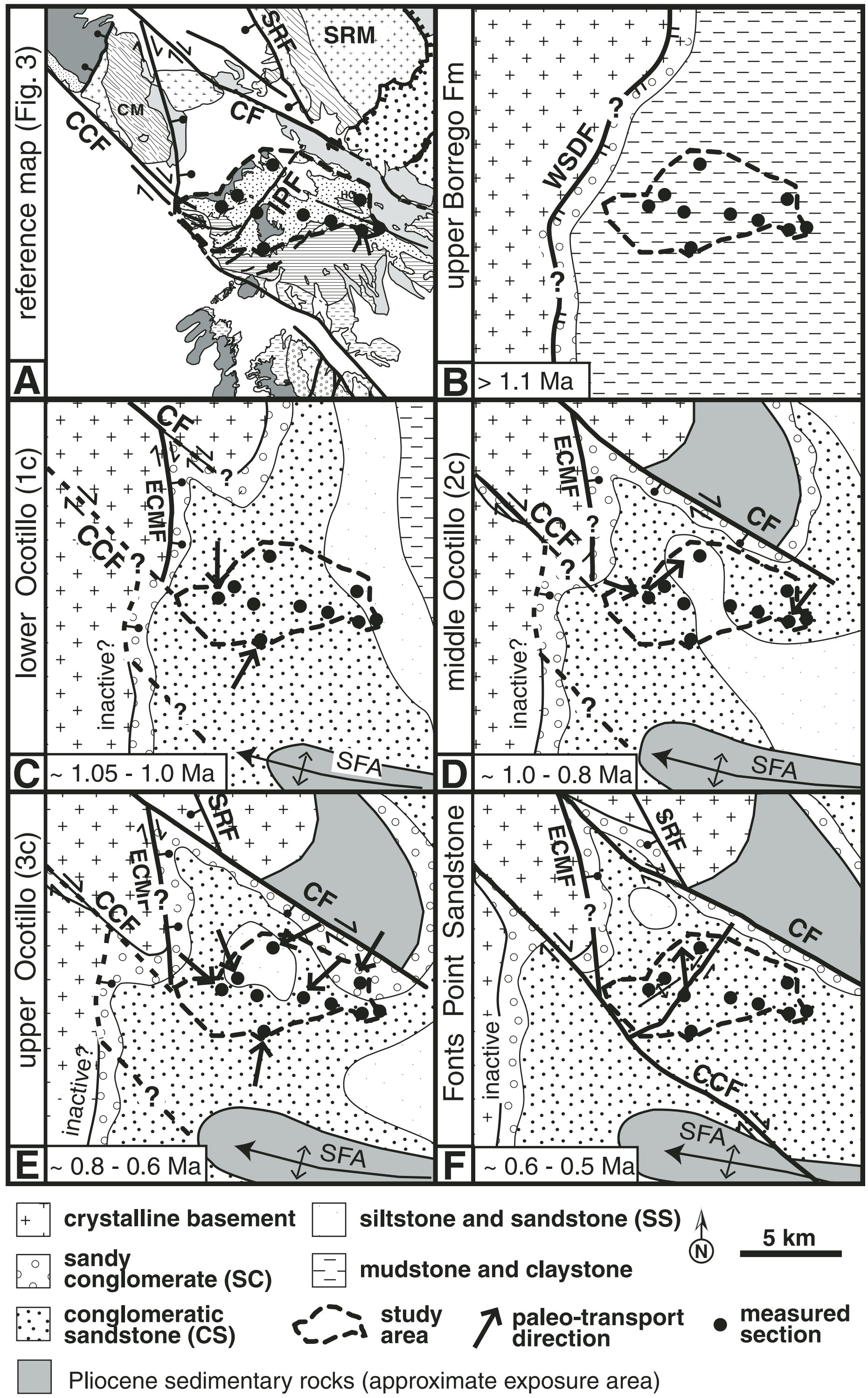

Figure 15. Paleogeographic reconstructions of the Borrego Badlands during deposition of the Ocotillo Formation and Fonts Point Sandstone. CCF—Coyote Creek fault; CF—Clark fault; ECMF—East Coyote Mountain fault; IPF—Inspiration Point fault; SFA—San Felipe anticline; SRF—Santa Rosa fault; SRM—Santa Rosa Mountains; WSDF—West Salton detachment fault. Patterns in panel A are explained in Figure 3. Faults indicated with dashed lines indicate uncertain interpretations. See text for discussion. Samples 1c, 2c, and 3c are coarse-grained facies of members 1, 2, and 3 of the Ocotillo Formation.

prior to deposition of the Ocotillo Formation, the Borrego Badlands was situated near the western margin of the regional Borrego Lake (Fig. 15B). Perennial lake conditions were abruptly terminated by base-level fall at ca. 1.1 Ma (Lutz, 2005; Kirby, 2005; Kirby et al., in press).

Deposition of Ocotillo member 1 took place from ca. 1.05 to 1.0 Ma, during rapid progradation of coarse alluvial sediment to the east, northeast, and south over much of the study area (Fig. 15C). Gravel was derived from crystalline source areas southwest and north of the basin. Initial progradation was followed by retreat of alluvial fans back toward basin margins, as recorded in finer-grained deposits of submember 1f (Figs. 7 and 8). The isopach map reveals a roughly N-trending, northward-deepening depocenter during deposition of member 1, with thinning to the west and east (Fig. 9A). This pattern is interpreted to record early growth of the East Coyote Mountain fault, and thus represents the earliest signal of slip on basin-bounding faults in the study area. The eastward lateral change from coarse alluvium to fine-grained lacustrine sediment in the eastern Borrego Badlands indicates that this area was contiguous with the eastward-retreating Borrego Lake. Lack of detrital input from the northeast shows that little or no high topography existed in the southern Santa Rosa Mountains during this time.

Ocotillo member 2 (ca. 1.0–0.8 Ma) records progradation of coarse alluvial sediment from multiple sources into a fluvial flood basin or shallow marshy palustrine depocenter (Fig. 15D). Member 2 contains the oldest detritus derived from the southern Santa Rosa Mountains, and thus records initial creation of topographic relief there. Increased input of coarse sediment from different sources was likely related to fault-related uplift around the basin margins. Isopach maps reveal the onset of NNE-ward thickening obliquely toward the Clark fault and away from the crest of the San Felipe anticline (Fig. 9B). New input from the northeast was related to oblique dextral slip and uplift along the Clark fault in the southern Santa Rosa Mountains (Fig. 15D).

Ocotillo member 3 (ca. 0.8–0.6 Ma) records strong progradation and deposition of coarse gravelly alluvium in the eastern part of the study area (Figs. 8 and 15E). Clastic sediment continued to enter the basin from the southwest and northwest, reducing the zone of fine-grained palustrine deposition to a small area surrounded by coarser sand flats and alluvial fans (Fig. 15E). Member 3 thus appears to record the earliest development of an internally drained subbasin, similar to but south of the modern Clark Dry Lake (Fig. 3). Clasts of reworked Diablo Formation sandstone become increasingly abundant in member 3 deposits, reflecting uplift and exhumation of the Palm Spring Group around the margins of the basin. Appearance of Diablo and marble clasts in the eastern sections, SW-directed paleocurrents, and strong progradational architecture all reflect increased topography in the southern Santa Rosa Mountains that we infer resulted from the vertical component of slip on the Santa Rosa segment of the Clark fault.

Deposition of the Fonts Point Sandstone (ca. 0.6–0.5 Ma) took place during overall northward transport and deposition of sandy alluvium in a thin sheet across the study area (Fig. 15F). This unit records the end of subsidence and a brief neutral period prior to the onset of modern uplift and erosion. The sub–Fonts Point angular unconformity northwest of the Inspiration Point fault records initial growth of northeast-trending folds and the Inspiration Point fault shortly prior to deposition of the Fonts Point Sandstone (Fig. 13).

DISCUSSION

Evolution of Basin-Bounding Faults and Folds

Data presented above provide new evidence for initiation and slip on basin-bounding faults in the Borrego Badlands, and one large intrabasinal fold, as described below.

San Felipe Anticline

The San Felipe anticline is a large, EW-trending fold in the San Felipe Hills that grew and segmented the San Felipe–Borrego basin during deposition of the Ocotillo Formation (Fig. 1) (Kirby, 2005; Kirby et al., in press). Growth of this anticline produced a widespread angular unconformity and disconformity at the base of the Ocotillo Formation, and was related to deactivation of the West Salton detachment fault and onset of dextral and oblique-slip faulting at or slightly before 1.1 Ma (Kirby et al., in press; Steely, 2006). South of Fonts Point to Borrego Mountain, the Fonts Point Sandstone rests on progressively older rocks of the Tertiary sedimentary section and underlying Cretaceous tonalite on the north limb of the W-plunging anticline (Fig. 3). This map pattern and stratigraphic thickness patterns indicate that, in combination with slip on the Clark fault, growth of the San Felipe anticline exerted a primary control on basin tilting and architecture of the Ocotillo Formation in the Borrego Badlands. The San Felipe anticline is now cut and offset by the Coyote Creek fault, suggesting that fold growth predates initiation of the Coyote Creek fault in the study area (see below).

Clark Fault

Stratigraphic data presented above show that the Santa Rosa segment of the Clark fault controlled basin subsidence and flanking topography at the northeast margin of the Borrego Badlands depocenter during deposition of Ocotillo member 2, at ca. 1.0 Ma. We interpret the lack of clastic input from the northeast in member 1 as indicating that member 1 predates propagation of the Clark fault to the surface here. While it is possible that this fault could have been active during late Borrego and early Ocotillo deposition, here we have shown that depositional facies, paleocurrents, grain size, clast composition, and stratigraphic thickness variations are all sensitive signals of fault activity that allow us to date initiation of the fault in this area. These signals are absent in member 1 near the Clark fault and appear in member 2, providing evidence for initiation of a faulted basin margin along the Clark fault by ca. 1.0 Ma.

In detail, paleocurrent and clast-composition data in the eastern Borrego Badlands (HC section; Fig. 7) appear inconsistent with our reconstruction for Ocotillo member 3 (Fig. 15E). Alluvial fan conglomerate in the upper Ocotillo Formation contains clasts of basement-derived mylonite and marble, and the paleocurrent data record transport to the southwest, which implies a basement source located northeast of the HC section. However, lithologies exposed northeast of the eastern Borrego Badlands today consist mainly of Canebrake Conglomerate (Fig. 3), which in this area is dominated by tonalite clasts with very few metamorphic basement rocks. Because the Santa Rosa Mountains have been translating to the southeast along the Clark fault since its initiation, they must be restored even farther away to the northwest relative to the HC section in Pleistocene time (Fig. 15E). This suggests that either sediment was transported to the southeast along the Clark fault prior to entering the basin, or Ocotillo member 3 was derived from rocks directly northeast of the eastern Borrego Badlands and was reworked from older, metamorphic clast-bearing conglomerate of the Palm Spring Group that has since been eroded away from the area immediately northeast of the fault. We prefer the latter interpretation based on the coarse, poorly sorted nature of member 3 conglomerate in this area.

Santa Rosa Fault

Stratal architecture and clast compositions in the Ocotillo Formation provide evidence for fault-controlled subsidence in the basin, and uplift northeast of the basin, during deposition of Ocotillo members 2 and 3. While these patterns can be attributed to slip on the Clark fault, uplift in the footwall of the Santa Rosa fault may have also contributed to high topography in the southern Santa Rosa Mountains during this time. The Santa Rosa fault is a young normal fault with very steep topographic relief, prominent triangular facets, and hanging valleys, and appears to be kinematically linked to the Clark fault (Figs. 1 and 3) (Dorsey, 2002; Ryter, 2002). Spatial association of the Clark and Santa Rosa faults suggests but does not require that both faults may have initiated at about the same time, during deposition of Ocotillo member 2.

East Coyote Mountain Fault

Our data provide indirect evidence for slip on the East Coyote Mountain fault during deposition of Ocotillo member 1, beginning at ca. 1.05 Ma. Subparallel alignment of roughly N-trending isopachs in member 1 with the East Coyote Mountain fault, and evidence for westward thinning of this unit (Figs. 7 and 9), imply that this fault controlled early subsidence and tilting in the basin. Young motion on this fault is likely based on the position of Clark Dry Lake immediately east of Coyote Mountain (Fig. 3), although the fault scarp is not fresh (Ryter, 2002). In any case, stratigraphic thickness trends and common occurrence of Coyote Mountain–type clasts in the AO and BW sections suggest that the East Coyote Mountain fault was active during deposition of Ocotillo member 1. This represents the earliest record of fault activity in the San Jacinto fault zone that is recognized in the Borrego Badlands.

Inspiration Point Fault

Initiation of the Inspiration Point fault and related NE-trending folds coincides closely in time with initial deposition of the Fonts Point Sandstone at ca. 0.6 Ma, as described above. The Coyote Creek fault appears to have propagated into the study area from the northwest at this time, during the onset of transpressive deformation and basin inversion. Initiation of slip on the Inspiration Point fault coincides with a major reorganization of the San Jacinto fault zone that initiated uplift and compressional deformation in both the Borrego Badlands (this study) and the San Felipe Hills (Kirby, 2005; Kirby et al., in press), and greatly slowed or terminated slip on dextral-normal strands of the San Felipe fault zone at the southwest margin of the basin (Steely, 2006).

Coyote Creek Fault

The timing of initiation of the Coyote Creek fault is difficult to assess because it cuts through the middle of the basin and does not occupy an emergent basin margin. However, there is no good evidence for slip on the Coyote Creek fault in the western Borrego Badlands during deposition of the Ocotillo Formation. SSW-ward stratigraphic thinning and increase in abundance of paleosols can be explained by tilting toward the Clark fault on the north limb of the San Felipe anticline, and does not require syn-Ocotillo movement on the Coyote Creek fault. Strata of the Ocotillo Formation do not display any lateral coarsening or thickening southwest of the BW section to within ~100 m of the Coyote Creek fault. Interbedded silicified tufa mounds at one locality close to a strand of the fault (Fig. 4) may indicate the presence of hot springs with possible fault control, but these are more likely to be related to slip on the East Coyote Mountain fault.

Importantly, the entire Ocotillo Formation is missing southwest of the Coyote Creek fault along an angular unconformity between more-folded Diablo Formation and less-folded Fonts Point Sandstone (Fig. 3) (Dibblee, 1984; Ryter, 2002). This relationship could be interpreted to mean that the Coyote Creek fault was active with a component of NE-side-down slip during deposition of the Ocotillo Formation. However, truncation of units beneath the Fonts Point Sandstone is best explained by north-northeast tilting on the north limb of the San Felipe anticline (Fig. 3), and so the lack of Ocotillo Formation does not require syn-Ocotillo slip on the fault. Moreover, the Coyote Creek fault presently displays NE-side-up displacement across fault scarps in the same area (Fig. 3) (Ryter, 2002; Sharp and Clark, 1972; this study). However, the Coyote Creek fault has SW-side-up offset at Borrego Mountain (Fig. 3), and it is common for strike-slip faults to reverse their vertical sense of offset, so we cannot assume a constant slip sense through time. Despite these complications, the lack of facies change toward the fault in the Ocotillo Formation, and compelling evidence for north-northeast tilting on the San Felipe anticline on both sides of the Coyote Creek fault prior to deposition of the Fonts Point Sandstone (Fig. 3), indicate that the Coyote Creek fault in the western Borrego Badlands initiated at ca. 0.6 Ma during a change from transtension that caused basin subsidence to transpressional deformation that uplifted and deformed the basinal deposits. We have reinterpreted Pleistocene sedimentary strata northwest of the study area in Coyote Canyon (Dorsey, 2002) to record slip on the Coyote Creek fault as early as ca. 0.8–1.0 Ma (Janecke et al., 2005), which suggests that the fault may have propagated southeast into the study area at ca. 0.6 Ma.

Timing and Cause of Ocotillo Progradation

The similar age of the basal Ocotillo Formation in widely dispersed locations around the southwestern Salton Trough (Brown et al., 1991; Kirby et al., in press; this study) provides evidence for very rapid progradation of coarse alluvial sediments over the former Borrego Lake at 1.05–1.07 Ma. This records a profound change in basin dynamics that requires abrupt slowing of subsidence and/or increase in sediment flux to the basin, and likely involves strong forcing by tectonic and/or climatic factors. Although we do not know the rate of sediment accumulation in the Borrego Formation and therefore cannot compare it to rates in the overlying Ocotillo Formation, the rapid rate of sedimentation in the lower Ocotillo Formation (1.4–3.9 mm/yr) likely exceeded that of the clay-rich upper Borrego Formation. If so, this would imply a positive correlation between grain size and sediment accumulation rate and would suggest that regional progradation was caused by an increase in sediment flux (e.g., Paola et al., 1992; Heller and Paola, 1992). However, it may be inappropriate to apply this type of analysis to the Borrego-Ocotillo transition because the contact is in many places an angular unconformity or disconformity, which indicates that a tectonic driving force needs to be considered.

In the Borrego Badlands, the basal Ocotillo contact changes from a short-lived hiatus in the west to an abrupt but conformable contact in the east (this study). In the San Felipe Hills, the contact is an angular unconformity over the San Felipe anticline and becomes a disconformity to conformable contact away from the fold crest (Kirby, 2005; Kirby et al., in press). Perennial lake conditions represented by the Borrego Formation were terminated across this contact, and when deposition resumed it took place in gravel-rich distal alluvial fans, sandy washes, and lake-margin fluvial-deltaic environments (Kirby, 2005; Kirby et al., in press). The drop in regional base level coincides with the appearance of abundant sandstone clasts reworked from the Pliocene Diablo Formation, which was eroded from previously subsiding southwestern parts of the extensional basin in the hanging wall of the detachment fault. Thus the data record a major tectonic reorganization in which the San Felipe and San Jacinto fault zones were initiated and the West Salton detachment fault became inactive, at or slightly prior to 1.1 Ma (Kirby, 2005; Kirby et al., in press; Steely, 2006; this study). Although the timing and nature of this reorganization are becoming clear, the controls on base-level fall that caused the abrupt change from lacustrine to alluvial sedimentation remain poorly understood. Possible mechanisms include crustal warping associated with initiation of strike-slip faults, changes in lithospheric buoyancy related to upper mantle processes, or changes in tectonically controlled regional drainage patterns in the southern Salton Trough.

This question remains unresolved and requires further study.

Some authors have proposed that late Cenozoic gravel progradation and increased sedimentation rates resulted from the onset of glacial climate oscillations and enhanced erosion starting at ca. 2–3 Ma (Zhang et al., 2001; Molnar, 2004). However, as noted by Kirby et al. (in press), we can reject the hypothesis that progradation of the Ocotillo Formation was caused primarily by climate forcing because (1) the age of the stratigraphic signal (ca. 1.1 Ma) is much younger than the change to a glacial climate regime at ca. 2.5–3.0 Ma, (2) paleoclimate studies in the southwestern United States record no major climate change at 1.1 Ma (Smith, 1984, 1994; Forester, 1991; Thompson, 1991; Zachos et al., 2001), and (3) climate change could not have produced the new basement uplifts, recycled clasts, angular unconformity in the San Felipe Hills (Dibblee, 1954; Kirby, 2005; Kirby et al., in press), and tilting and thickening of the Ocotillo Formation in the Borrego Badlands (this study).

Age of the San Jacinto Fault

In this paper and two companion studies (Steely, 2006; Kirby et al., in press), we present compelling evidence that the San Jacinto and San Felipe faults initiated in the western Salton Trough at ca. 1.1 Ma, or possibly slightly earlier if there was a time lag between initial fault motion and transfer of the signal into the basin. The age of active faults is useful for determining long-term (geologic) slip rates and thus is important for estimating earthquake recurrence and seismic hazards. Here we focus on the timing of fault initiation, since a full discussion of slip rates at different time scales is beyond the scope of this paper. Our results are consistent with those of Morton and Matti (1993) and Matti and Morton (1993), who used evidence from Pleistocene deposits in the San Timoteo Badlands to estimate an age of ca. 1.2–1.5 Ma for initiation of the San Jacinto fault near its northwest end where it merges with the San Andreas fault (Fig. 1A). They inferred that the San Jacinto fault formed as a result of increasing structural complexity, crustal convergence, and resistance to strike-slip motion through San Gorgonio Pass, a major restraining bend between the Coachella Valley and Mojave segments of the San Andreas fault. An age of ca. 1.2–1.5 Ma in the northwest is only slightly older than the ca. 1.1 Ma age of the San Jacinto fault zone in the western Salton Trough, and suggests that fault initiation was virtually synchronous or propagated very rapidly from northwest to southeast. Importantly, our work confirms the young age of the San Jacinto fault as determined near its northwest end (Morton and Matti, 1993; Matti and Morton, 1993; Albright, 1999). An older age of ca. 2.4 Ma, which is based on extrapolation of previously estimated Quaternary slip rates (Merifield et al., 1989; Rockwell et al., 1990), is not supported by any evidence that we know of and is unlikely based on our improved knowledge of the geologic record.

CONCLUSIONS

Pleistocene sedimentary rocks in the Borrego Badlands provide a high-resolution record of fault-related deposition in the San Jacinto fault zone between ca. 1.1 and 0.6 Ma. The Ocotillo Formation contains lithofacies ranging from conglomerate and sandstone deposited in alluvial fans to mudstone and siltstone that accumulated in low-energy floodplain and marshy palustrine environments. The base of the Ocotillo Formation is dated with magnetostratigraphy, tephrochronology, and previous studies of vertebrate paleontology at 1.05 ± 0.03 Ma. Synchronous progradation of Ocotillo gravel over a large area in the San Felipe–Borrego basin apparently resulted from initiation of dextral strike-slip faults and related folds in the western Salton Trough at ca. 1.1 Ma (Kirby, 2005; Kirby et al., in press; Steely, 2006; this study).

North-trending isopachs in Ocotillo member 1 suggest that the East Coyote Mountain fault controlled basin tilting starting about 1.05 Ma. Facies architecture, thickness trends, and distribution of paleosols in members 2 and 3 record the onset of tilting toward the north-northeast at ca. 1.0 Ma, toward the Clark fault and away from the growing San Felipe anticline. Starting at this time, the southern Santa Rosa Mountains became an area of high topography that shed voluminous coarse detritus into the basin from the northeast. The data thus provide multiple lines of evidence that slip on the Santa Rosa segment of the Clark fault began at ca. 1.0 Ma.

Facies architecture and thickness variations in the western Borrego Badlands provide no compelling evidence for slip on the Coyote Creek fault in the study area during deposition of the Ocotillo Formation. The sheetlike Fonts Point Sandstone overlies the tilted Tertiary section along an angular unconformity that progressively truncates the entire Tertiary section south of Fonts Point to Borrego Mountain. The map data thus indicate that, in combination with slip on the Clark fault, growth of the San Felipe anticline exerted a primary control on basin tilting, filling, and erosion during deposition of the Ocotillo Formation in the Borrego Badlands.

The base of the Fonts Point Sandstone changes from conformable in a 1 to 2 km wide belt southeast of the Inspiration Point fault to an angular unconformity northwest of the fault. Using the 0.74 Ma Thermal Canyon ash and a sedimentation rate of 0.32–0.42 mm/yr in the upper Ocotillo Formation, we calculate an age of 0.6 ± 0.02 Ma for the base of the Fonts Point Sandstone. This dates initiation of the Inspiration Point and Coyote Creek faults, and onset of folding, uplift, and erosion in the Borrego Badlands. The timing of this event is nearly identical to the end of deposition and onset of transpressive deformation in the San Felipe Hills (Kirby, 2005; Kirby et al., in press). Thus we conclude that the onset of deformation in the Borrego Badlands coincides with a major structural reorganization in the western Salton Trough that established the modern geometry and kinematics of the San Jacinto fault zone at ca. 0.6 Ma.

ACKNOWLEDGMENTS

We thank Gary Petro, Noel Liner, Amy Fluette, and Kurt Heim for assistance with the paleomagnetic study. Gary Girty, Rick Bennett, and John Fletcher are thanked for insightful and constructive reviews of this paper. Our research benefited from conversations with Gary Axen, George Jefferson, Todd LaMaskin, Jarg Pettinga, Greg Retallack, Tom Rockwell, Derek Ryter, and Ray Weldon. George Jefferson provided access to field and laboratory resources in Anza-Borrego Desert State Park. We thank Jeff Johnson for help with GIS technology and assistance in the field. This study was supported by grants from the National Science Foundation: EAR-0125921 to Dorsey, EAR-0125454 to Housen, and EAR-0125497 to Janecke. The cryogenic magnetometer at Western Washington University was provided by NSF grant EAR-9727032 to Housen.

REFERENCES CITED

Albright, L.B., III, 1999, Magnetostratigraphy and biochronology of the San Timoteo Badlands, Southern California, with implications for local Pliocene-Pleistocene tectonic and depositional patterns: Geological Society of America Bulletin, v. 111, p. 1265–1293, doi: 10.1130/0016-7606(1999)111<1265:MABOTS>2.3.CO;2.

Axen, G.J., and Fletcher, J.M., 1998, Late Miocene-Pliocene extensional faulting, northern Gulf of California, Mexico, and Salton Trough, California: International Geology Review, v. 40, no. 3, p. 219–244.

Bartholomew, M.J., 1968, Geology of the southern portion of the Fonts Point quadrangle and the southwestern portion of the Seventeen Palms quadrangle, San Diego County, California [M.S. thesis]: Los Angeles, University of Southern California, 60 p.

Bartholomew, M.J., 1970, San Jacinto fault zone in the northern Imperial Valley, California: Geological Society of America Bulletin, v. 81, p. 3161–3166.

Bell, C.J., Lundelius, E.L., Barnosky, A.D., Graham, R.W., Lindsay, E.H., Ruez, D.R., Jr., Semken, H.A., Jr., Webb, S.D., and Zakrzewski, R.J., 2004, The Blancan, Irvingtonian, and Rancholabrean mammal ages, *in* Woodburne, M.O., ed., Late Cretaceous and Cenozoic mammals of North America: Biostratigraphy and geochronology: New York, Columbia University Press, p. 232–314.

Bennett, R.A., Rodi, W., and Reilinger, R.E., 1996, Global positioning system constraints on fault slip rates in Southern California and northern Baja, Mexico: Journal of Geophysical Research, B, Solid Earth and Planets, v. 101, p. 21,943–21,960.

Birkeland, P.W., 1999, Soils and geomorphology: New York, Oxford University Press, 430 p.

Blair, T.C., 1987a, Sedimentary processes, vertical stratification sequences, and geomorphology of the Roaring River alluvial fan, Rocky Mountain National Park, Colorado: Journal of Sedimentary Petrology, v. 57, no. 1, p. 1–18.

Blair, T.C., 1987b, Tectonic and hydrologic controls on cyclic alluvial fan, fluvial, and lacustrine rift-basin sedimentation, Jurassic–lowermost Cretaceous Todo Santos Formation, Chiapas, Mexico: Journal of Sedimentary Petrology, v. 57, no. 5, p. 845–862.

Blair, T.C., and McPherson, J.G., 1994, Alluvial fans and their natural distinction from rivers based on morphology, hydraulic processes, sedimentary processes, and facies assemblages: Journal of Sedimentary Research, v. 64, no. 3, p. 450–489.

Bogen, N.L., and Seeber, L., 1986, Neotectonics of rotating blocks within the San Jacinto fault zone, Southern California: Eos (Transactions, American Geophysical Union), v. 67, p. 1200.

Brown, N.N., Fuller, M.D., and Sibson, R.H., 1991, Paleomagnetism of the Ocotillo Badlands, Southern California, and implications for slip transfer through an antidilational fault jog: Earth and Planetary Science Letters, v. 102, no. 3–4, p. 277–288, doi: 10.1016/0012-821X(91)90023-B.

Buchheim, H.P., Brand, L.R., and Goodwin, H.T., 2000, Lacustrine to fluvial deposition in the Eocene Bridger Formation: Palaeogeography, Palaeoclimatology, Palaeoecology, v. 162, no. 1–2, p. 191–209, doi: 10.1016/S0031-0182(00)00112-7.

Calzia, J.P., McGuire, D.J., Oliver, H.W., and Schreiner, R.A., 1988, Mineral resources of the Santa Rosa Mountains Wilderness study area, Riverside County, California: U.S. Geological Survey Bulletin 1710, p. D1–D14.

Cande, S.C., and Kent, D.V., 1995, Revised calibration of the geomagnetic polarity timescale for the Late Cretaceous and Cenozoic: Journal of Geophysical Research, B, Solid Earth and Planets, v. 100, no. 4, p. 6093–6095.

Collinson, J.D., 1996, Alluvial sediments, *in* Reading, H.G., ed., Sedimentary environments: processes, facies and stratigraphy: London, Blackwell Science, p. 37–82.

DeMets, C., and Dixon, T., 1999, New kinematic models for Pacific–North America motion from 3 Ma to present, 1: Evidence for steady motion and biases in the NUVEL-1A model: Geophysical Research Letters, v. 26, p. 1921–1924, doi: 10.1029/1999GL900405.

DeMets, C., Gordon, R.G., Argus, D.F., and Stein, S., 1990, Current plate motions: Geophysical Journal International, v. 101, p. 425–478.

Dibblee, T.W., Jr., 1954, Geology of the Imperial Valley region, California, *in* Jahns, R.H., ed., Geology of Southern California: California Department of Natural Resources, Division of Mines Bulletin 170, p. 21–28.

Dibblee, T.W., Jr., 1984, Stratigraphy and tectonics of the San Felipe Hills, Borrego Badlands, Superstition Hills, and vicinity, *in* Rigsby, C.A., ed., The Imperial Basin: Tectonics, sedimentation, and thermal aspects: Field Trip Guidebook—Pacific Section, Society of Economic Paleontologists and Mineralogists, v. 40, p. 31–44.

Dibblee, T.W., Jr., 1996, Stratigraphy and tectonics of the Vallecito–Fish Creek Mountains, Vallecito Badlands, Coyote Mountains, and Yuha Desert, southwestern Imperial Desert, *in* Abbott, P.L., and Seymour, D.C., eds., Sturzstroms and detachment faults, Anza-Borrego Desert State Park, California: South Coast Geological Society Guidebook No. 24, p. 59–79.

Dorsey, R.J., 2002, Stratigraphic record of Pleistocene initiation and slip on the Coyote Creek fault, lower Coyote Creek, Southern California, *in* Barth, A., ed., Contributions to crustal evolution of the southwestern United States: Geological Society of America Special Paper 365, p. 251–269.

Dorsey, R.J., 2006, Stratigraphy, tectonics, and basin evolution in the Anza-Borrego Desert region, *in* Jefferson, G.T., and Lindsay, L.E., eds., Fossil treasures of the Anza-Borrego Desert: San Diego, California, Sunbelt Publications, p. 89–104.

Dorsey, R.J., and Roering, J.J., 2006, Quaternary landscape evolution in the San Jacinto fault zone, Peninsular Ranges of Southern California: Transient response to strike-slip fault initiation: Geomorphology, v. 73, no. 1–2, p. 16–32, doi: 10.1016/j.geomorph.2005.06.013.

Dorsey, R.J., Janecke, S.U., Kirby, S.M., McDougall, K.A., and Steely, A.N., 2005, Pliocene evolution of the lower Colorado River in the Salton Trough: Tectonic controls on paleogeography and the regional Borrego Lake, *in* Reheis, M.C., ed., Geologic and biotic perspectives on late Cenozoic drainage history of the southwestern Great Basin and lower Colorado River region: Conference abstracts: U.S. Geological Survey Open-File Report 2005-1404, p. 13.

Dorsey, R.J., Fluette, A., McDougall, K.A., Housen, B.A., Janecke, S.U., Axen, G.J., and Shirvell, C.R., in press, Chronology of Miocene-Pliocene deposits at Split Mountain Gorge, Southern California: A record of regional tectonics and Colorado River evolution: Geology, doi: 10.1130/G23139A.1.

Dronyk, M.P., 1977, Stratigraphy, structure, and a seismic refraction survey of a portion of the San Felipe Hills, Imperial Valley, California [M.S. thesis]: Riverside, University of California, 141 p.

Eberth, D.A., and Miall, A.D., 1991, Stratigraphy, sedimentology and evolution of a vertebrate-bearing, braided to anastamosed fluvial system, Cutler Formation (Permian-Pennsylvanian), north-central New Mexico: Sedimentary Geology, v. 72, no. 3–4, p. 225–252, doi: 10.1016/0037-0738(91)90013-4.

Engel, A.E.J., and Schultejann, P.A., 1984, Late Mesozoic and Cenozoic history of south-central California: Tectonics, v. 3, no. 6, p. 659–675.

Ferragen, E.S., 1986, Geology of the southeastern San Felipe Hills, Imperial Valley, California [M.S. thesis]: San Diego, California, San Diego State University, 144 p.

Forester, R.M., 1991, Pliocene climate history of the western United States derived from lacustrine ostracods: Quaternary Science Reviews, v. 10, no. 2–3, p. 133–146, doi: 10.1016/0277-3791(91)90014-L.

Gastil, R.G., 1975, Plutonic zones in the Peninsular Ranges of Southern California and northern Baja California: Geology, v. 3, p. 361–363, doi: 10.1130/0091-7613(1975)3<361:PZITPR>2.0.CO;2.

Gawthorpe, R.L., Fraser, A.J., and Collier, R.E., 1994, Sequence stratigraphy in active extensional basins: Implications for the interpretation of ancient basin-fills: Marine and Petroleum Geology, v. 11, p. 642–658, doi: 10.1016/0264-8172(94)90021-3.

Gawthorpe, R.L., Sharp, I., Underhill, J.R., and Gupta, S., 1997, Linked sequence stratigraphic and structural evolution of propagating normal faults: Geology, v. 25, p. 795–798, doi: 10.1130/0091-7613(1997)025<0795:LSSASE>2.3.CO;2.

Gile, L.H., Hawley, J.W., and Grossman, R.B., 1981, Soils and geomorphology in the Basin and Range area of southern New Mexico; guidebook to the desert project: Socorro, New Mexico, New Mexico Bureau of Mines and Mineral Resources Memoir 39, 222 p.

Guthrie, L.L., 1990, An internally standardized study of Cenozoic sand and sandstone compositions, Salton Basin, Southern California: Implications for rift basin evolution with emphasis on the Palm Spring and Imperial Formations [M.S. thesis]: San Diego, California, San Diego State University, 180 p.

Heller, P.L., and Paola, C., 1992, The large-scale dynamics of grain-size variation in alluvial basins, 2: Application to syntectonic conglomerate: Basin Research, v. 4, p. 91–102.

Heward, A.P., 1978, Alluvial fan sequence and megasequence models; with examples from Westphalian D–Stephanian B coalfields, *in* Miall, A.D., ed., Fluvial sedimentology: Calgary, Canada, Canadian Society of Petroleum Geologists Memoir 5, p. 669–702.

Hoover, R.A., 1965, Areal geology and physical stratigraphy of a portion of the northern Santa Rosa Mountains, San Diego County, California [M.A. thesis]: Riverside, University of California, 81 p.

Horng, C., Lee, M., Palike, H., Wei, K., Liang, W., Iizuka, Y., and Torii, M., 2002, Astronomically calibrated ages for geomagnetic reversals within the Matuyama Chron: Earth, Planets, and Space, v. 54, no. 6, p. 679–690.

Housen, B.A., Dorsey, R.J., Janecke, S.U., Kirby, S.M., and Lutz, A.T., 2004, Magnetostratigraphy and rotation of Pleistocene sedimentary rocks in the San Jacinto fault zone, western Salton Trough, CA: Eos (Transactions, American Geophysical Union), v. 85, p. 671.

Jahns, R.H., 1954, Geology of the Peninsular Range province, Southern California and Baja California (Mexico), *in* Jahns, R.H., ed., Geology of Southern California: California Department of Natural Resources, Division of Mines Bulletin 170, p. 29–52.

Janecke, S.U., Kirby, S.M., Langenheim, V.E., Steely, A.N., Dorsey, R.J., Housen, B., and Lutz, A.T., 2005, High geologic slip rates on the San Jacinto fault zone in the SW Salton Trough, and possible near-surface slip deficit in sedimentary basins: Geological Society of America Abstracts with Programs, v. 37, no. 7, p. 275.

Jefferson, G.T., 2001, Paleontological resources management, Anza-Borrego Desert State Park, *in* Santucci, V.L., and McClelland, L., eds., Proceedings of the 6th Fossil Resource Conference; 2001, a fossil odyssey: Technical Report—National Park Service, Geological Resource Division: Grand Junction, Colorado, p. 137–166.

Jefferson, G.T., and Remeika, P., 1994, The mid-Pleistocene stratigraphic co-occurrence of *Mammuthus columbi* and *M. imperator* in the Ocotillo Formation, Borrego Badlands, Anza-Borrego Desert State Park, California: Current Research in the Pleistocene, v. 11, p. 89–92.

Kendrick, K.J., Morton, D.M., Wells, S.G., and Simpson, R.W., 2002, Spatial and temporal deformation along the northern San Jacinto fault, Southern California: Implications for slip rates: Bulletin of the Seismological Society of America, v. 92, p. 2782–2802, doi: 10.1785/0120000615.

Kerr, D.R., 1982, Early Neogene continental sedimentation, western Salton Trough, California [M.S. thesis]: San Diego, California, San Diego State University, 134 p.

Kerr, D.R., and Kidwell, S.M., 1991, Late Cenozoic sedimentation and tectonics, western Salton Trough, California, *in* Walawender, M.J., and Hanan, B.B., eds., Geological excursions in Southern California and Mexico: San Diego, California, San Diego State University, p. 397–416.

Kirby, S.M., 2005, The Quaternary structural and tectonic evolution of the San Felipe Hills, CA [M.S. thesis]: Logan, Utah State University, 3 plates, 181 p.

Kirby, S.M., Janecke, S.U., Dorsey, R.J., Housen, B.A., Langenheim, V., McDougall, K., and Steely, A.N., in press, Initial strike slip deformation along the San Felipe and San Jacinto fault zones, Southern California, constrained by the Pleistocene Brawley and Ocotillo formations: Journal of Geology.

Langenheim, V.E., and Jachens, R.C., 1993, Isostatic residual gravity map of the Borrego Valley 1:100,000-scale quadrangle, California: U.S. Geological Survey Open-File Report 93-246, 1 sheet.

Lutz, A.T., 2005, Tectonic controls on Pleistocene basin evolution in the central San Jacinto fault zone, Southern California [M.S. thesis]: Eugene, University of Oregon, 136 p.

Mack, G.H., and Seager, W.R., 1990, Tectonic control on facies distribution of the Camp Rice and Palomas Formations (Pliocene-Pleistocene) in the southern Rio Grande rift: Geological Society of America Bulletin, v. 102, p. 45–53, doi: 10.1130/0016-7606(1990)102<0045:TCOFDO>2.3.CO;2.

Martin, A.J., 1999, Geophysical characterization of the upper Borrego Valley, San Diego County, California [M.S. thesis]: Long Beach, California State University, 259 p.

Matti, J.C., and Morton, D.M., 1993, Paleogeographic evolution of the San Andreas fault in Southern California: A reconstruction based on a new cross-fault correlation, *in* Powell, R.E., et al., eds., The San Andreas fault system: Displacement, palinspastic reconstruction, and geologic evolution: Geological Society of America Memoir 178, p. 107–159.

McCaffrey, R., 2005, Block kinematics of the Pacific–North America plate boundary in the southwestern United States from inversion of GPS, seismological, and geologic data: Journal of Geophysical Research, v. 110, p. B07401, doi: 10.1029/2004JB003307.

Meade, B.J., and Hager, B.H., 2005, Block models of crustal motion in Southern California constrained by GPS measurements: Journal of Geophysical Research, v. 110, p. B03403, doi: 10.1029/2004JB003209.

Merifield, P.M., Rockwell, T.K., Loughman, C.C., and Klinger, R.E., 1989, Study of seismic activity by selective trenching along the San Jacinto fault zone, Southern California: Santa Monica, California, Lamar-Merifield, Geologists, Report 89-1, 30 p.

Miall, A.D., 1978, Lithofacies types and vertical profile models in braided river deposits: A summary, *in* Miall, A.D., ed., Fluvial sedimentology: Calgary, Canada, Canadian Society of Petroleum Geologists Memoir 5, p. 597–604.

Michaelsen, P., Henderson, R.A., Crosdale, P.J., and Mikkelsen, S.O., 2000, Facies architecture and depositional dynamics of the Upper Permian Rangal coal measures, Bowen basin, Australia: Journal of Sedimentary Research, v. 70, no. 4, p. 879–895.

Molnar, P., 2004, Late Cenozoic increase in accumulation rates of terrestrial sediment: How might climate change have affected erosion rates?: Annual Reviews of Earth and Planetary Science, v. 32, p. 67–89, doi: 10.1146/annurev.earth.32.091003.143456.

Morley, E.R., 1963, Geology of the Borrego Mountain quadrangle and the western portion of the Shell Reef quadrangle, San Diego County, California [M.S. thesis]: University of Southern California, 138 p.

Morton, D.M., and Matti, J.C., 1993, Extension and contraction within an evolving divergent strike-slip fault complex: The San Andreas and San Jacinto fault zones at their convergence in Southern California, *in* Powell, R.E., et al., eds., The San Andreas fault system: Displacement, palinspastic reconstruction, and geologic evolution: Geological Society of America Memoir 178, p. 217–230.

Paola, C., 2000, Quantitative models of sedimentary basin filling: Sedimentology, v. 47, Supplement 1, p. 121–178, doi: 10.1046/j.1365-3091.2000.00006.x.

Paola, C., Heller, P.L., and Angevine, C.L., 1992, The large-scale dynamics of grain-size variation in alluvial basins, 1: Theory: Basin Research, v. 4, p. 73–90.

Pettinga, J.R., 1991, Structural styles and basin margin evolution adjacent to the San Jacinto fault zone, Southern California: Geological Society of America Abstracts with Programs, v. 23, no. 5, p. 257.

Quinn, H.A., and Cronin, T.M., 1984, Micropaleontology and depositional environments of the Imperial and Palm Spring Formations, Imperial Valley, California, *in* Rigsby, C.A., ed., The Imperial Basin: Tectonics, sedimentation, and thermal aspects: Los Angeles, California, Pacific Section, Society of Economic Paleontologists and Mineralogists, p. 71–85.

Reitz, D.T., 1977, Geology of the western and central San Felipe Hills, northwestern Imperial County, California [M.S. thesis]: Los Angeles, University of Southern California, 155 p.

Remeika, P., 1998, Interdisciplinary age control of the western Borrego Badlands, Anza-Borrego Desert State Park, California, The 5th Conference on Fossil Resources 1998, Partners Preserving our Past Planning our Future: Conference on Fossil Resources—Abstracts with Programs: Grand Junction, Colorado, U.S. Department of Agriculture Forest Service, p. S18.

Remeika, P., 2006, Dating, ashes, and magnetics: New times for old bones, *in* Jefferson, G.T., and Lindsay, L.E., eds., Fossil treasures of the Anza-Borrego Desert: San Diego, California, Sunbelt Publishers, p. 107–119.

Remeika, P., and Beske-Diehl, S., 1996, Magnetostratigraphy of the western Borrego Badlands, Anza-Borrego State Park, California: Implications for stratigraphic age control, *in* Abbott, P.L., and Seymour, D.C., eds., Sturzstroms and detachment faults, Anza-Borrego Desert State Park, California: South Coast Geological Society Guidebook No. 24, p. 209–220.

Remeika, P., and Jefferson, G.T., 1993, The Borrego local fauna: Revised basin-margin stratigraphy and paleontology of the western Borrego Badlands, Anza-Borrego Desert State Park, California, *in* Reynolds, R.E., and Reynolds, J., eds., Ashes, faults, and basins: Redlands, California, San Bernardino County Museum Association, San Bernardino County Museum Association Special Publication, p. 90–93.

Remeika, P., and Pettinga, J.R., 1991, Stratigraphic revision and depositional environments of the middle to late Pleistocene Ocotillo Conglomerate, Borrego Badlands, Anza-Borrego Desert State Park, California: Abstracts from the Symposium on the Scientific Value of the Desert, Anza Borrego Foundation, Borrego Springs, California, p. 13.

Retallack, G.J., 2001, Soils of the Past: Oxford, UK, Blackwell Press, 404 p.

Rockwell, T.K., Loughman, C.C., and Merifield, P.M., 1990, Late Quaternary rate of slip along the San Jacinto fault zone near Anza, Southern California: Journal of Geophysical Research, B, Solid Earth and Planets, v. 95, no. 6, p. 8593–8605.

Rogers, T.H., 1965, Geologic map of California, Santa Ana sheet: California Division of Mines and Geology, scale 1:250,000, 2 sheets.

Rust, B.R., and Koster, E.H., 1984, Coarse alluvial deposits, *in* Walker, R.G., ed., Facies models: Toronto, Geological Society of Canada. P. 53–69.

Ryter, D.W., 2002, Late Pleistocene kinematics of the central San Jacinto fault zone, Southern California [Ph.D. thesis]: Eugene, University of Oregon, 137 p.

Sanders, C.O., 1989, Fault segmentation and occurrence in the strike-slip San Jacinto fault zone, California, *in* Schwartz, D.P., and Sibson, R.H., eds., Proceedings of Conference XLV: A workshop on fault segmentation and controls of rupture initiation and termination: U.S. Geological Survey Open-File Report 89-0315, p. 324–349.

Sanders, C.O., and Magistrale, H., 1997, Segmentation of the northern San Jacinto fault zone, Southern California: Journal of Geophysical Research, B, Solid Earth and Planets, v. 102, no. 12, p. 27,453–27,467, doi: 10.1029/97JB02377.

Sarna-Wojcicki, A.M., Meyer, C.E., and Wan, E., 1997, Age and correlation of tephra layers, position of the Matuyama-Brunhes chron boundary, and effects of Bishop ash eruption on Owens Lake, as determined from drill hole OL-92, southeastern California, *in* Smith, G.I., and Bischoff, J.L., eds., An 800,000-year paleoclimatic record from core OL-92, Owens Lake, southeastern California: Geological Society of America Special Paper 317, p. 79–90.

Sarna-Wojcicki, A.M., Pringle, M.S., and Wijbrans, J., 2000, New $^{40}Ar/^{39}Ar$ age of the Bishop Tuff from multiple sites and sediment rate calculation for the Matuyama-Brunhes boundary: Journal of Geophysical Research, B, Solid Earth and Planets, v. 105, no. 9, p. 21,431–21,443, doi: 10.1029/2000JB900091.

Scheuing, D.F., and Seeber, L., 1991, Magnetostratigraphy of Neogene sediments in the San Jacinto fault zone, Southern California, and paleomagnetic evidence for block rotation: American Association of Petroleum Geologists Bulletin, v. 75, no. 3, p. 666–667.

Scheuing, D.F., Seeber, L., and Van Fossen, M., 1991, Structural and sedimentological effects on detrital paleomagnetic directions and their bearing on Neogene block rotation in the San Jacinto fault zone, Southern California: Eos (Transactions, American Geophysical Union), v. 71, p. 1632.

Sharp, R.V., 1967, San Jacinto fault zone in the Peninsular Ranges of Southern California: Geological Society of America Bulletin, v. 78, p. 705–730.

Sharp, R.V., 1981, Variable rates of late Quaternary strike slip on the San Jacinto fault zone, Southern California: Journal of Geophysical Research, B, Solid Earth and Planets, v. 86, no. 3, p. 1754–1762.

Sharp, R.V., and Clark, M.M., 1972, Geologic evidence of previous faulting near the 1968 rupture on the Coyote Creek Fault, *in* The Borrego Mountain earthquake of April 9, 1968: U.S. Geological Survey Professional Paper 787, p. 131–140.

Simpson, C., 1984, Borrego Springs–Santa Rosa mylonite zone: A Late Cretaceous west-directed thrust in Southern California: Geology, v. 12, p. 8–11, doi: 10.1130/0091-7613(1984)12<8:BSRMZA>2.0.CO;2.

Singer, B., and Brown, L.L., 2002, The Santa Rosa event: $^{40}Ar/^{39}Ar$ and paleomagnetic results from the Valles rhyolite near Jaramillo Creek, Jemez Mountains, New Mexico: Earth and Planetary Science Letters, v. 197, no. 1–2, p. 51–64, doi: 10.1016/S0012-821X(01)00598-2.

Smith, G.A., 1994, Climatic influences on continental deposition during late-stage filling of an extensional basin, southeastern Arizona: Geological Society of America Bulletin, v. 106, p. 1212–1228, doi: 10.1130/0016-7606(1994)106<1212:CIOCDD>2.3.CO;2.

Smith, G.I., 1984, Paleohydrologic regimes in the southwestern Great Basin, 0–32 my ago, compared with other long records of "global" change: Quaternary Research, v. 22, no. 1, p. 1–17, doi: 10.1016/0033-5894(84)90002-4.

Steely, A.N., 2006, The evolution from Pliocene West Salton detachment faulting to cross-cutting Pleistocene oblique strike-slip faults in the SW Salton Trough, Southern California [M.S. thesis]: Logan, Utah State University, 239 p.

Steely, A.N., Janecke, S.U., Axen, G.J., and Dorsey, R.J., 2005, Pleistocene (~1 Ma) transition from West Salton detachment faulting to cross-cutting dextral strike-slip faults in the SW Salton Trough: Geological Society of America Abstracts with Programs, v. 37, no. 7, p. 274.

Tarbet, L.A., and Holman, W.H., 1944, Stratigraphy and micropaleontology of the west side of Imperial Valley, California: American Association of Petroleum Geologists Bulletin, v. 28, no. 12, p. 1781–1782.

Theodore, T.G., and Sharp, R.V., 1975, Geologic map of the Clark Lake quadrangle, San Diego County, California: U.S. Geological Survey Miscellaneous Field Studies Map MF-644, scale 1:24,000, 1 sheet.

Thompson, R.S., 1991, Pliocene environments and climates in the western United States: Quaternary Science Reviews, v. 10, no. 2–3, p. 115–132, doi: 10.1016/0277-3791(91)90013-K.

Turkmen, I., and Kerey, I.E., 2000, Alluvial and lacustrine facies of the Yenicubuk Formation (lower-middle Miocene), upper Kizilirmak basin, Turkiye (Turkey), *in* Gierlowski, E.H., and Kelts, K.R., eds., Lake basins through space and time: AAPG studies in geology: Tulsa, Oklahoma, American Association of Petroleum Geologists, p. 449–463.

Wagoner, J.L., 1977, Stratigraphy and sedimentation of the Pleistocene Brawley and Borrego Formations in the San Felipe Hills area, Imperial Valley, California, U.S.A. [M.S. thesis]: Riverside, University of California, 128 p.

Wells, D.L., 1987, Geology of the eastern San Felipe Hills, Imperial Valley, California: Implications for wrench faulting in the southern San Jacinto fault zone [M.S. thesis]: San Diego, California, San Diego State University, 140 p.

Wells, S.G., and Dohrenwend, J.C., 1985, Relict sheetflood bed forms on late Quaternary alluvial-fan surfaces in the southwest United States: Geology, v. 13, p. 512–516, doi: 10.1130/0091-7613(1985)13<512:RSBFOL>2.0.CO;2.

Winker, C.D., 1987, Neogene stratigraphy of the Fish Creek–Vallecito section, Southern California: Implications for early history of the northern Gulf of California and the Colorado Delta [Ph.D. thesis]: University of Arizona, 494 p.

Winker, C.D., and Kidwell, S.M., 1996, Stratigraphy of a marine rift basin: Neogene of the western Salton Trough, California, *in* Abbott, P.L., and Cooper, J.D., eds., Field conference guidebook and volume for the American Association of Petroleum Geologists annual convention, p. 295–336.

Woodard, G.D., 1963, The Cenozoic succession of the west Colorado Desert, San Diego and Imperial Counties, Southern California [Ph.D. thesis]: Berkeley, University of California, 173 p.

Woodard, G.D., 1974, Redefinition of Cenozoic stratigraphic column in Split Mountain Gorge, Imperial Valley, California: American Association of Petroleum Geologists Bulletin, v. 58, no. 3, p. 521–526.

Zachos, J., Pagani, M., Sloan, L., Thomas, E., and Billups, K., 2001, Trends, rhythms, and aberrations in global climate 65 Ma to present: Science, v. 292, no. 5517, p. 686–693, doi: 10.1126/science.1059412.

Zhang, P., Molnar, P., and Downs, W.R., 2001, Increased sedimentation rates and grain sizes 2–4 Myr ago due to the influence of climate change on erosion rates: Nature, v. 410, no. 6831, p. 891–897, doi: 10.1038/35073504.

Manuscript Received 6 December 2005
Revised Manuscript Received 23 June 2006
Manuscript Accepted 10 July 2006

Printed in the USA